ANL-76-57

ANL-76-57

FINAL REPORT ON THE SMALL-SCALE VAPOR-EXPLOSION EXPERIMENTS USING A MOLTEN NaCl-H_2O SYSTEM

by

R. P. Anderson and L. Bova

BASE TECHNOLOGY

U of C-AUA-USERDA

ARGONNE NATIONAL LABORATORY, ARGONNE, ILLINOIS

Prepared for the U. S. ENERGY RESEARCH AND DEVELOPMENT ADMINISTRATION under Contract W-31-109-Eng-38

Printed in the United States of America
Available from
National Technical Information Service
U. S. Department of Commerce
5285 Port Royal Road
Springfield, Virginia 22161
Price: Printed Copy $4.00; Microfiche $3.00

Distribution Category:
LMFBR Safety (UC-79p)

ANL-76-57

ARGONNE NATIONAL LABORATORY
9700 South Cass Avenue
Argonne, Illinois 60439

FINAL REPORT ON THE SMALL-SCALE VAPOR-EXPLOSION EXPERIMENTS USING A MOLTEN NaCl-H_2O SYSTEM

by

R. P. Anderson and L. Bova

Reactor Analysis and Safety Division

April 1976

TABLE OF CONTENTS

LIST OF FIGURES

LIST OF TABLES

FINAL REPORT ON THE SMALL-SCALE VAPOR-EXPLOSION EXPERIMENTS USING A MOLTEN NaCl-H_2O SYSTEM

by

R. P. Anderson and L. Bova

ABSTRACT

Vapor explosions were produced by injecting small quantities of water into a container filled with molten NaCl. Minimum explosion efficiencies, as evaluated from reaction-impulse measurements, were relatively large. Subsurface movies showed that the explosions resulted from a two-step sequence: an initial bulk-mixing phase in which the two liquids intermix on a large scale, but remain locally separated by an insulating gas-vapor layer; and a second step, immediately following breakdown of the gas layer, during which the two liquids locally fragment, intermix, and pressurize very rapidly. The experimental results were compared with various mechanistic models that had been proposed to explain vapor explosions. Early models seemed inconsistent with the results. More recent theories suggest that vapor explosions may be caused by a nucleation limit or by dynamic mixing combined with high surface-heat-transfer rates. Both types of models are consistent with the results.

I. INTRODUCTION

Mixtures of hot and cold liquids will occasionally produce a violent explosion due to the sudden vaporization of the cold liquid. The phenomenon, generally termed a vapor explosion, has become recognized as a cause of accidents in an increasingly wide variety of industries during the last few years. To evaluate the potential hazards of vapor explosion associated with accidental contact between liquid masses at widely different temperatures, a safety analyst must answer two fundamental questions: Will the hypothesized liquid-liquid contact produce an explosion? How much energy would such an explosion release if it did occur? Sections A and B below will review the information that was available to answer these two questions at the inception of the current experimental program.

A. When Does Liquid-Liquid Contact Lead to an Explosion?

Two different approaches have been used to answer questions of this type. One approach tabulated conditions that had previously led to actual

vapor explosions and, on the basis of this experience, specified potentially "dangerous" and "safe" large-scale mixing conditions. The other approach attempted to derive a theoretical model of the explosion process that could be used to calculate the initial conditions that would lead to an explosion. Let us consider in more detail the answers each approach could derive from the early, available information.

Experience with actual accidents seemed to indicate that the explosions occurred on a somewhat random basis. Only about 5% of the cases in which pipe ruptures leaked cooling water into a paper-processing smelt furnace actually produced explosions.[1] On the other hand, the vast majority of foundry incidents in which molten metal has been spilled into water containers produced no energetic interaction, though the occasional explosion that did occur could be very destructive. (See Ref. 2 for a description of a particularly violent foundry accident.)

It was impossible to differentiate between safe and dangerous mixing conditions based on such seemingly random events. Accordingly, two early series of experimental studies were conducted using molten-aluminum-water systems[3] and smelt-water systems;[4] their goal was an explanation of the variable behavior. Results of the molten-aluminum-water studies did indeed show that certain macroscopic mixing conditions would not lead to explosions in that particular system, and as a result, changes in plant procedures were recommended which drastically reduced the incidence of vapor-explosion accidents in the aluminum-processing industry. Unfortunately, this type of approach did not work for all systems; equivalent "safe" operating conditions were not found for a smelt-water system, so that smelt furnaces were still subject to occasional explosions following rupture of a containing-water-coolant line. Another disadvantage to this system, which based safety predictions on past experience, is its inability to draw any meaningful conclusions about a new liquid pair for which there is no previous operating history. For example, the safety of molten-UO_2-Na systems could not be assessed using this approach.

A successful attempt to base explosion predictions on a theoretical model would have to assume that the physical mechanisms that initiated a vapor explosion were fully understood and would then have to use this fundamental understanding to perform a two-step calculation: First, the microscopic interface conditions that were necessary and sufficient to initiate an explosion would be evaluated; second, these microscopic conditions would be related to macroscopic mixing conditions. In practice, all such attempts broke down at the first step, since there was insufficient experimental information to prove which of the various hypothesized initiating mechanisms were valid. All such mechanisms had been postulated to account for the fact that vapor explosions must produce vapor at extremely high rates in order to generate shock waves. The latent heat for this vaporization must come from the hot liquid and must be readily available to the cold liquid during the rapid

vaporization. Such ready availability could be the result of a sudden large increase in the interfluid heat-transfer rates due to a rapid fragmentation and intermixing of the two liquids. Early workers in the field hypothesized one of four physical mechanisms causing such fragmentation:

1. The frozen-shell hypothesis suggested that the hot fluid formed a frozen shell around the cold fluid. As the heat continued to transfer between liquids, the shell thickened, and the cold fluid heated up until its vapor pressure was high enough to burst the frozen shell. This minor explosion fragmented and intermixed the liquids, generating a much larger explosion.

2. Cold-liquid entrainment assumed that droplets of the cold liquid infiltrated fissures in a freshly frozen crust of hot material or in the incoming liquid jet of hot material. In either case, the cold liquid suddenly boiled and initiated fragmentation.

3. Fragmentation was caused by the forces involved in the periodic collapse and reestablishment of a vapor film during transition boiling.

4. The last proposed mechanism was a Weber-type jet instability in which one liquid jetted into another, became unstable, and fragmented when the disruptive forces of viscous drag and momentum overcame the cohesive surface forces.

An alternative explanation for vapor explosions bypassed the problem of explaining a very rapid, fine fragmentation process by assuming that the heat was transferred into the cold liquid at a moderate rate, but that boiling initiation was delayed until a large amount of available heat was stored in the cold fluid in a nonequilibrium state well above the normal vaporization temperature.

There was no body of experimental facts that could be used to judge the validity of these various mechanistic models. Without valid proof that one of the postulated mechanisms was the actual initiating cause of vapor explosions, it was impossible to build a theoretical model for evaluating the explosion probability in a given situation.

B. How Much Energy Would Be Released during a Vapor Explosion?

The ultimate goal in assessing explosive energy release was a model capable of predicting the actual rate at which available thermal energy was converted to destructive mechanical energy during the total interaction period. However, due to the lack of physical understanding, such detailed calculations were impossible, and the analyst had to settle for models based on simplifications of one sort or another. Two different analytical approaches were tried, each based on a different set of simplifying assumptions.

The thermodynamic approach[5] specified equations of state for both liquids and calculated the net energy change in the system as it went through

a hypothesized sequence of processes. Loss of internal energy during this sequence was assumed to be available for conversion into destructive work. An upper bound could be placed on the conversion efficiency by hypothesizing the most conservative possible sequence of processes. In practice, this meant a two-process sequence followed by the working fluid: a constant-volume transfer of heat between the two liquids until an equilibrium temperature was reached, followed by an expansion back to ambient pressure with both fluids remaining in thermodynamic equilibrium throughout the expansion. This approach had to assume that equilibrium conditions existed at all times and had to ignore the actual rate processes involved in the phenomena.

A second theoretical approach tried to include the effects of heat-transfer rates by considering a very simplified physical picture which was analytically tractable. Typical models of this type were published in Refs. 6 and 7. They assumed that, before the calculations were started, a mixture of the two liquids was already in existence in the form of a matrix of discrete particles of one fluid dispersed in a continuum of the other fluid. The behavior of the system was calculated as it expanded against known physical constraints with energy transport between the liquids optionally specified by either conduction or convection equations. The models allowed for parametric variation of the particle diameter and spacing, mass ratio of the two fluids in the mixing zone, heat-transfer mode, and an arbitrarily assigned delay period in the initial dispersion time.

The physical insight gained from studying the effects of the parametric variations on system behavior was extremely valuable. However, the models were not suitable for calculating the maximum energy-conversion rate, since not enough was understood about the conditions leading to initial explosion geometry so that the parametric values could be correctly evaluated for known examples. If one assumed the worst case in evaluating the parameters, the model predictions must revert back to the answers derived from the thermodynamic calculations.

Again, there were no actual measurements of explosive energy release to compare with either the theoretical maximum-work output as calculated by the thermodynamic approach or the energy-conversion rates as calculated by the various rate models.

There was a very apparent need for an experimental program supplying facts to help answer two specific questions: What mechanism (or mechanisms) provides the initiating trigger for a vapor explosion? How efficiently does a vapor explosion convert thermal energy to mechanical energy?

II. EXPERIMENTAL PLAN

At the inception of these experiments, very few measurements were available either to test the validity of hypothesized initiating mechanisms for vapor explosion or to determine explosive energy release. An experimental program was set up to fill this void. The original plan called for a parametric study to measure variation in vapor-explosion intensity when fluid properties and mixing techniques were changed.

It was decided that the initial experiments should be conducted using small quantities of the hot and cold liquids, thus simplifying both the techniques for handling and mixing the two fluids at widely different temperatures and the techniques for making measurements. A necessary second step in this program would require running tests with larger liquid volumes to ensure that small-scale results would apply to large-scale systems.

The experiments were conceptually simple: A pair of liquids that were known to explode were chosen; a few cubic centimeters of the cold liquid were injected into a small container filled with the hot liquid (typical volume, 50-100 cm^3). Measurements of reaction force and pressure taken during and after the explosion were to be used in conjunction with reaction liquid volumes, either determined from known injection rates or scaled off of individual movie frames, to calculate energy release and conversion efficiency for each test. Variations in explosion intensity from test to test were to be used to construct a table showing the parametric relationship between explosion intensity and changes in both the system geometry (location and speed of the cold-liquid injection) and the properties of the two liquids (temperature, surface tension, dissolved gas content, etc.). Selected tests were to be conducted with a transparent hot liquid contained in a transparent crucible so that the subsurface interfluid mixing could be recorded on high-speed movies. The various mechanistic explosion theories were to be judged against the data bank contained in both the movies and the table.

The mixing geometry for the first series of tests consisted of a cold-liquid jet which penetrated through the surface and into the bulk of hot liquid. These first tests produced a number of unexpected results. It was found that there were at least three distinct types of liquid-liquid interactions ranging in size from a mild type akin to boiling to a very rapid, high-pressure explosion. The intensity of the explosions did not vary smoothly from one type to the next; instead, the system acted as though it were tristable, with three discrete levels of kinetic-energy production. Small, uncontrolled fluctuations in physical properties or mixing dynamics would shift the system from one explosion level to another. Obviously the original goal of a table showing a smooth functional relationship between the control parameters, and the explosive energy release had to be abandoned.

Additional tests were conducted with the same equipment, searching for the cause of the apparently random shifts in system behavior. Eventually

the inconsistency was traced to the behavior of a gas layer between the two liquids during a preexplosive mixing stage. The gas layer controlled the location and size of a small preliminary interaction whose subsequent turbulent aftermath occasionally entrapped cold-liquid droplets in the hot fluid, producing large energetic explosions.

The equipment was redesigned to run a second series of tests which attempted to control the geometry of the two liquids and the intervening gas layer so as to produce large explosions in a clean, turbulent-free system. The following sections of this report describe the experimental equipment, outline the experimental results, and interpret their meaning. Each section is divided into two parts dealing separately with the original planned parametric study and the second series of tests which investigated efficient explosions in controlled geometries.

III. EXPERIMENTAL EQUIPMENT AND PROCEDURE

A. Parametric Study

The experimental program was originally planned as a parametric study to show the dependence of the explosion intensity upon a number of controlled variables. In keeping with this basic purpose, the equipment emphasized ease and speed of operation, so that a large number of variables could be investigated in a reasonable period. Early scoping experiments had been conducted to test the explosive productivity of a number of hot and cold liquid pairs contacted in various geometric configurations.[8] Results from these tests gave valuable guidance in answering three major questions that arose during the conceptual design stages of the present study: Which two liquids should be contacted? What liquid volumes and overall system geometry should be used? What meaningful measurements could be made?

In choosing the hot and cold liquids to be used in the test program, we placed prime importance on the absolute certainty that the two liquids could be made to explode when mixed in small quantities. It was known that liquid pairs that readily exploded when mixed in large volumes might not explode at all when mixed in small volumes. For example, explosions had been produced from both accidental and deliberate contact between large volumes of molten aluminum and water, but these results could not be reproduced by pouring together small volumes of the two liquids in a normal laboratory environment.[9] Scoping experiments had identified a number of liquid pairs which exploded when mixed in small quantities under laboratory conditions. Various molten salts and water formed the most consistently explosive pairs and also met the additional experimental requirement that both liquids had to be transparent, so that the subsurface mixing process could be recorded on high-speed movies. Molten NaCl and water were selected as the most suitable liquid pair for this test program.

The size and geometry of the liquid-liquid contacting system were also selected on the basis of results from the scoping experiments that produced explosions by injecting few-gram quantities of water through a hypodermic needle into a crucible containing about 100 g of molten salt. (Note that no explosions were ever produced using the inverse geometry with small-diameter jets of hot liquid penetrating into a bulk mass of cold liquid.) The final equipment design for the present series of tests was essentially an automated version of the equipment used in the scoping experiments. Shown in simplified schematic form as Fig. 1, the test apparatus operated as follows: A $1\frac{1}{2}$-in.-wide, 1-in.-deep, 2-in.-high crucible, containing about 80 g of NaCl, was placed in an induction coil. The salt was first melted and then heated to a preselected temperature. At that time, an automatic control system was activated. It sequentially:

1. Shut off the induction generator.

2. Energized an air cylinder, which lowered the base support plate for the dual purpose of furnishing a rigid base for high-frequency

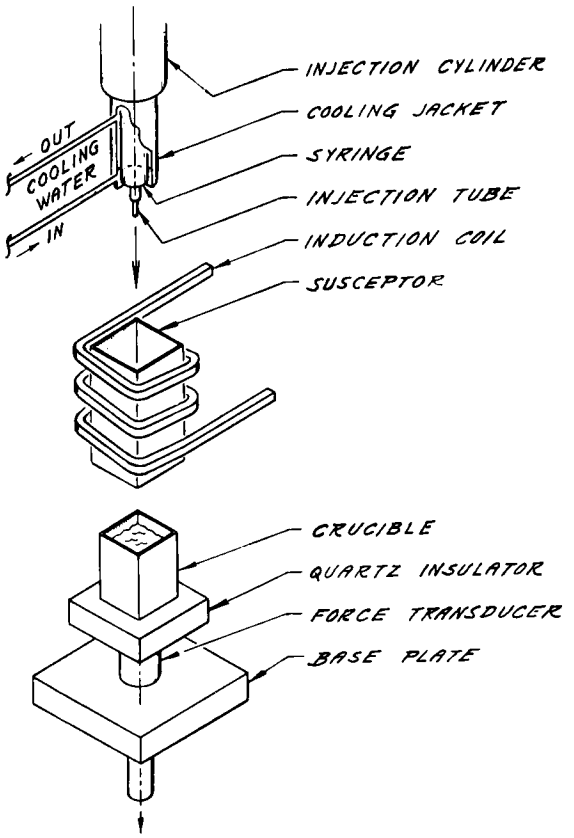

Fig. 1. Isometric View of Experimental Equipment. ANL Neg. No. 900-4485.

force-transducer measurements and bringing the crucible into optical viewing range.

3. Pressurized another air cylinder, which lowered the water-injection syringe into position.

4. Turned on the high-intensity lights, high-speed camera, and instrument-recording system.

5. Pressurized a third air cylinder, which injected water from a cooled hypodermic syringe through an 18-gauge needle (0.035-in. ID) into the molten-salt bath.

The initial tests were to be run in stainless steel crucibles which could easily be fabricated. Then, based on those results, it was planned to duplicate selected runs in quartz crucibles which would allow subsurface, high-speed movies.

Measurements included salt and water temperatures preceding the injection, a load-cell measurement of the vertical reaction force during the explosion, and high-speed movies of the system during the whole period (starting before the injection process and finishing well after any interactions were completed).

Injection-water temperature was controlled by adjusting the temperature of the water that circulated through the cooling jacket around the injection syringe and needle assembly.

A retractable sheathed thermocouple monitored the temperature at one salt-bath location while the salt was melting and the liquid was heating above the melt temperature. Calibration tests with thermocouples in various salt-bath locations had measured a temperature gradient of about 3°C/sec during the cooling period following withdrawal of the salt bath from the induction-heating coil. Thus the actual temperature of the salt bath at the time of injection could be calculated from the initial temperature measurement and the known delay period between lowering the power input to the induction coil and injecting the water.

The piezoelectric force transducer used in this equipment had a natural resonant frequency of 40,000 Hz. As installed, however, other lower

frequencies became dominant. The crucible and insulating quartz block were supported on the transducer, which in turn was mounted on a rigid base plate (see Fig. 1). The effect was similar to a damped spring-mass system whose measured response characteristics showed a major oscillation at 1800 Hz and another, much smaller, oscillation at 5000 Hz. Details of the pressure rise occurring faster than about a quarter wavelength of the dominant frequency [$\tau = 1/(4 \times 1800 \text{ cps}) = 0.00014$ sec] would be lost in the instrumentation system. However, the total impulse due to a short-period load (impulse is defined as the time integral of the force) should be accurately represented by the area under the recorded force curve. When calibration tests were run with known impulsive loads, the measurements deviated less than 5% from the known input.

Movies were taken with a 16-mm, rotating-prism camera using a 35-mm lens; 2500 frames/sec were recorded on Kodak Tri-X reversal film. Reflective lighting was supplied by three 1-kW quartz iodide lamps. To protect the lights and camera, the experimental equipment was enclosed in a blastproof box constructed of 1/4-in.-thick aluminum plates and 1/2-in.-thick Plexiglas viewports.

In summary, explosions were to be produced by injecting a few grams of water in the form of a 0.035-in.-dia jet into an 80-g mass of molten sodium chloride. Salt and water temperatures were to be controlled and measured. The experimental apparatus was contained in a blastproof aluminum box with Plexiglas view ports for high-intensity lights and a high-speed movie camera, which recorded preexplosive mixing and postexplosive expansion. The impulse due to the vertical reaction forces during an actual explosion was measured by a piezoelectric force transducer whose output signal was recorded on an FM magnetic-tape unit. A photograph of the assembled system is shown in Fig. 2.

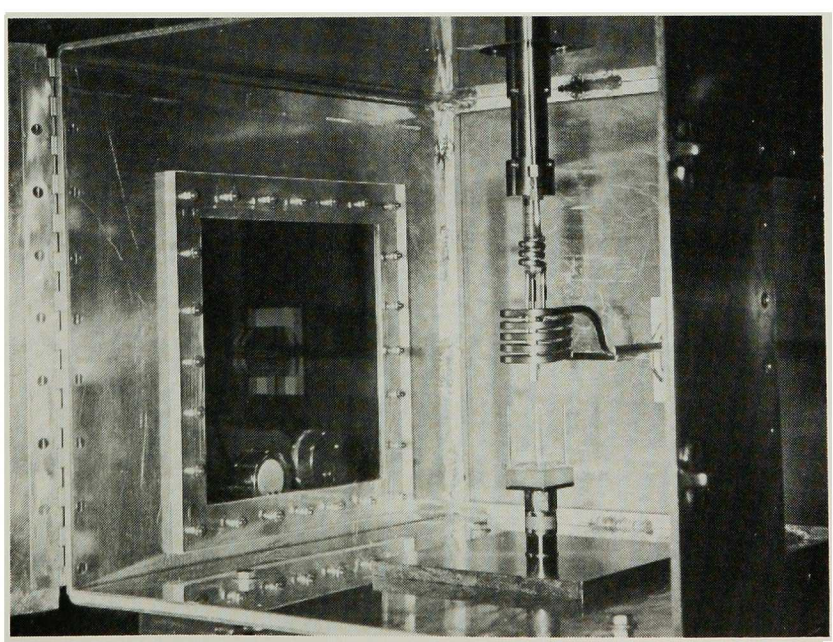

Fig. 2. Photographic View of Experimental Equipment

B. Controlled-geometry Tests

The goal of the controlled-geometry tests was to initiate large vapor explosions by suddenly introducing a small quantity of water below the surface of a molten salt mass in a system free from entrapped gases and turbulent mixing currents. Only one major change was necessary to convert the equipment from its original design for the parametric study. The above technique for the injection of water, which had caused gas entrainment and turbulent mixing in the parametric tests, had to be replaced with some system for quietly and quickly injecting water below the salt surface.

The first attempts used water-filled, thin-glass spheres, which were rapidly injected into the salt bath. The spheres were allowed to break from internal pressure generated by the heated water or else were deliberately broken by being smashed into the bottom of the crucible. Both methods were tried and failed to produce explosions, so the whole concept was abandoned.

A second injection technique returned to the use of an injection needle, but lowered the needle tip below the salt surface after the salt was molten and immediately preceding the injection of water. Large quantities of water vapor boiled from the stainless steel needle as it was submerged into the molten-salt bath, causing many of the same problems as in above-surface injection tests. Successive attempts to improve the system by increasing the insulation around the needle finally resulted in a successful test which used a needle constructed of concentric quartz tubes with an insulating gas layer between them.

IV. EXPERIMENTAL RESULTS

A. Parametric Results

The major features of the present equipment were patterned after that used in early scoping experiments which had unfailingly produced explosions when water was injected into molten salt. It was expected that explosions would also be readily produced in the current equipment. The overall plan was to roughly measure the dependence of explosion intensity on initial parameter variation using stainless steel crucibles, and then to go back and make more refined measurements using quartz crucibles which allowed subsurface movies of the pre-explosive mixing. It was hoped that the movies might also be fast enough to detect variations in the initiation and growth of the explosion itself.

In the first five tests 3 cm^3 of 14°C water (in the form of a 0.035-in. jet with a velocity of ~50 ft/sec) were injected into 80 g of molten sodium chloride at temperatures ranging from 880 to 980°C (NaCl melts at 800°C). Contrary to expectations, these tests failed to produce a large explosion; instead, they generated mild interactions which quietly splashed the salt out of the crucible. The interactions were delayed until some time after the initial jet penetration into the salt mass, with the delay periods ranging from 10 to 30 msec.

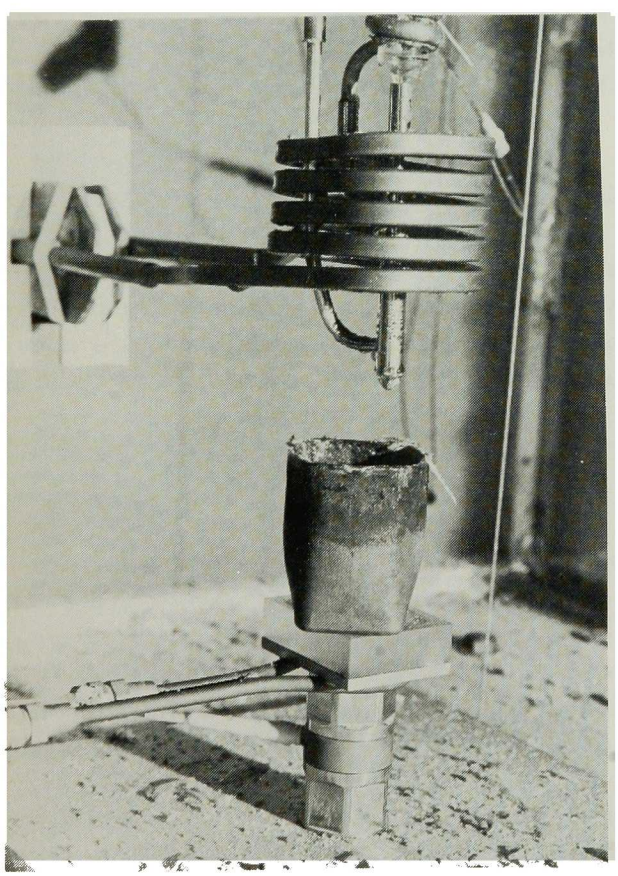

Fig. 3. View of Test Equipment Showing Salt Dispersion and Crucible Distortion Caused by a Large, Delayed Explosion

The sixth attempt resulted in a violent explosion. The force-link record and high-speed movies were lost due to a failure in the timing mechanism, but the rapid high pressurization was evident from the distortion of 1/16-in.-wall stainless steel crucible (see Fig. 3). The observers noted subjectively that the delay period between the water injection and the interaction appeared to be longer in this test than it had been in the previous five tests.

Efforts to reproduce this explosion by duplicating its initial controlled conditions failed during the next four tests. Uncontrolled variations in the temperature gradients and turbulence levels within the water jet seemed the most likely causes of the

behavioral differences between tests run with duplicate initial conditions. As an indirect proof of this hypothesis, a series of experiments was conducted at various injection pressures to investigate the effect of changes in the jet characteristics upon system behavior. Twenty tests were run with injection pressures ranging between 60 and 16 psig; all produced mild interactions with typical short delay times between the water injection and the interactions. Finally four tests, run at 8-psig injection pressure, resulted in different reactions. One of these tests again produced only a mild interaction following a short initial delay period, but the other three tests, with longer initial delay periods, generated two intermediate-sized interactions and another very violent explosion, which distorted the stainless steel crucible. Five more tests, run at 7-psia injection pressure, produced one early small interaction and four delayed reactions--two of medium size and two of the large violent type.

These subjective observations of delay periods and explosion intensities were verified by the experimental measurements and movies. Figure 4 is composed of selected cinema frames showing the movement of the upper salt surface following high-pressure injection of a water jet. As may be seen, an initial upward surface splash was starting to recede when the effects of a sudden interaction blew most or all of the salt out of the crucible. This interaction occurred 27 msec after the jet first entered the crucible and appeared on the load-cell trace as a small, sharp signal which forced the load cell to ring at its natural mounted frequency.

As mentioned in Sec. III.A, the instrument system could not distinguish the fine details in the time variation of the vertical loading force, but the integral under the recorded curve was an accurate measurement of the total impulse from the actual load. These impulses were not a direct measurement of mechanical-energy release, which depended on both the explosive force and the reaction mass that this force acts upon; however, the impulse was used to calculate a lower limit of the actual mechanical-energy output by assuming the interaction occurred beneath the total salt mass. The procedure is outlined in Appendix A.

Figures 5 and 6 picture the movement of the upper salt surface for low-injection-pressure tests which produced delayed medium- and large-scale explosions, respectively. Though it is difficult to detect, in these few selected frames, actual viewing of both movies showed a slow change in the velocity of the salt mass, indicating a very small interaction, at about the same time that an interaction occurred in the earlier tests with higher jet speeds. Following this small intial interaction, there was a long delay period when the movies gave no indication of any events inside the crucible; then suddenly a medium or large explosion occurred. The initial interactions were too small to detect on the load-cell trace; the impulse from the medium-sized explosion was measured as 0.041 lb_F-sec and the large explosion gave a 0.714-lb_F-sec impluse measurement.

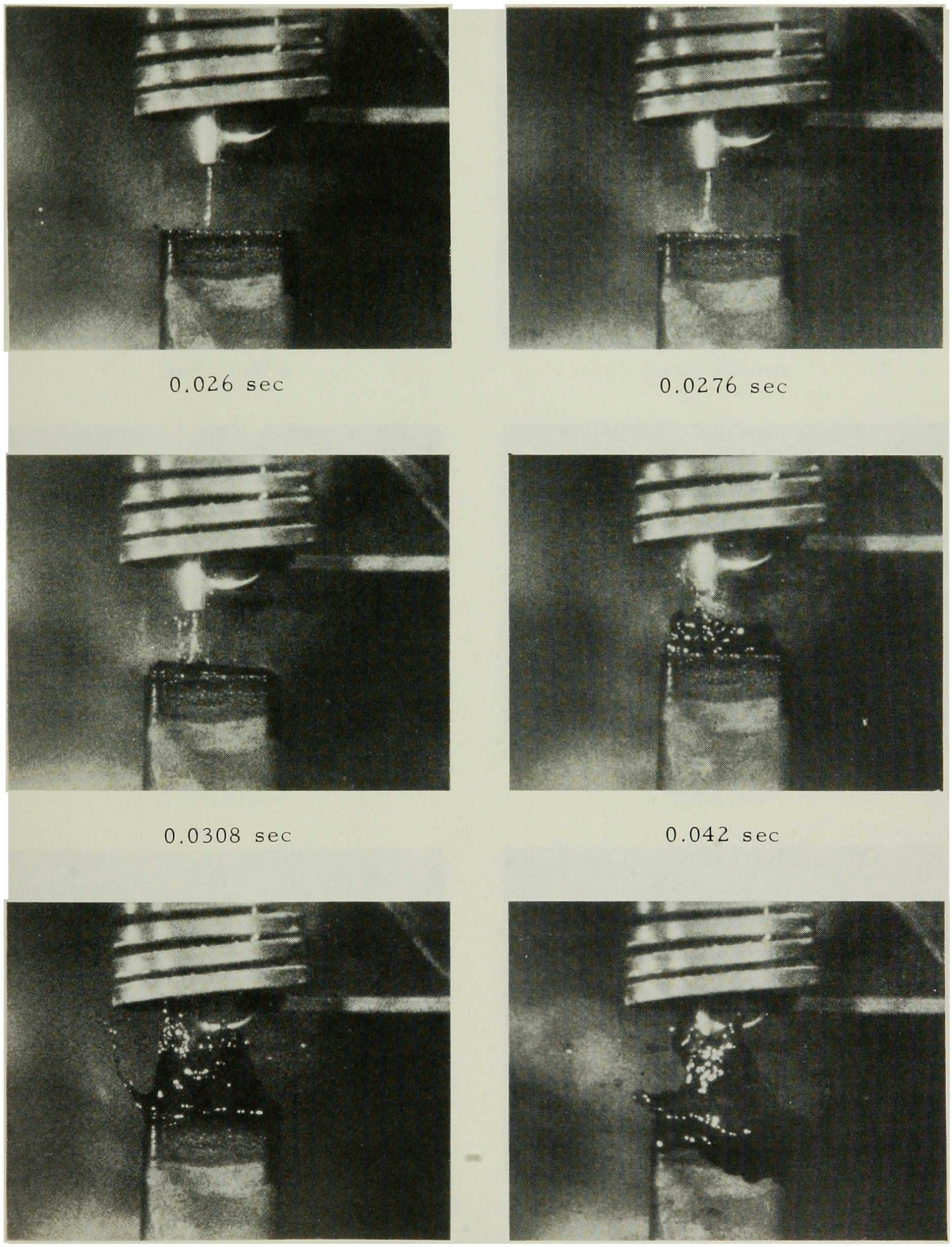

Fig. 4. Selected Movie Frames Showing a Typical Small NaCl-H_2O Interaction in a Stainless Steel Crucible. ANL Neg. No. 900-4501 Rev. 1.

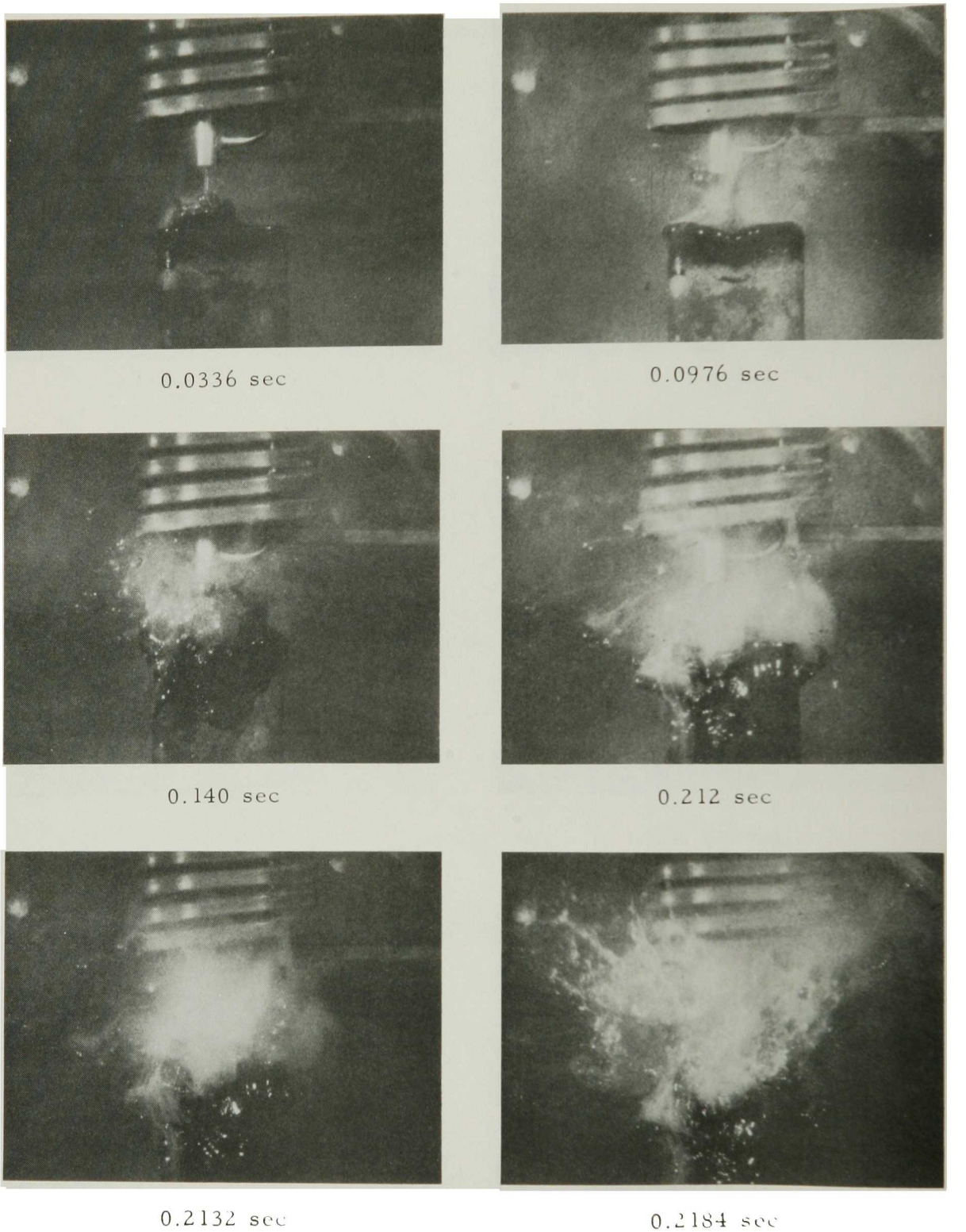

Fig. 5. A Delayed, Medium-scale Interaction in a Stainless Steel Crucible. ANL Neg. No. 900-4500 Rev. 1.

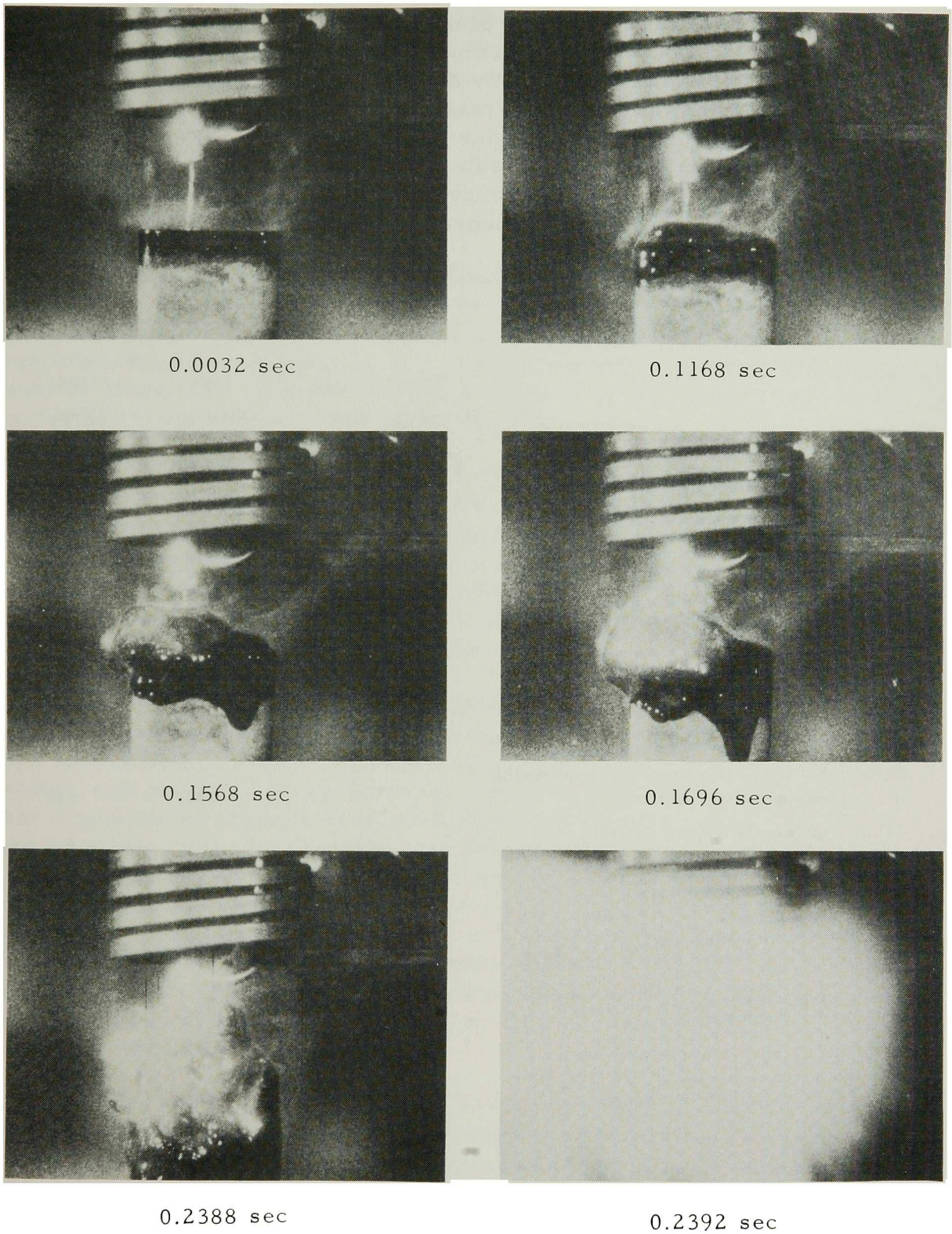

Fig. 6. A Delayed, Large Explosion in a Stainless Steel Crucible. ANL Neg. No. 900-4496 Rev. 1.

An upper limit to the amount of mechanical work produced per unit mass of injected working fluid (water) could be evaluated by a thermodynamic approach described in Appendix B. By multiplication of this upper limit by the known water-injection rates, the maximum theoretical work production could be assessed at any given time during a specific test. For each of the three tests pictured in Figs. 4-6. Table I lists the initial experimental conditions, the minimum mechanical energy release as calculated from the impulse measurement, the maximum theoretical system work production, and a

TABLE I. Energy Account for Tests with Above-surface Injection of Water into Molten NaCl Contained in a Stainless Steel Crucible

Explosion Characteristics			
Time:	Early	Late	Late
Intensity:	Small	Medium	Large
Salt temperature at time of explosion, T_{in}, °C	850	940	915
Energy in 80 g of NaCl at T_{in}, cal			
Heat in molten NaCl above melt = $mc_p(T_{in} - T_{freeze})$	1,096	3,069	2,521
Heat of fusion = mh_{sf}	9,280	9,280	9,280
Heat in solid NaCl above temperature of boiling water = $mc_p(T_{freeze} - T_{f_{H_2O}})$	14,224	14,224	14,224
Total energy in the NaCl, cal	24,600	26,573	26,025
Injection pressure, psig	8	8	7
Time delay between water-jet penetration and explosion initiation, msec	27	212	242
Volume of injected water at time of explosion initiation, cm^3	0.13	0.80	0.91
Theoretical work/mass assuming water undergoes constant-volume heating and constant-temperature expansion at the salt-bath temperature (see Appendix B), cal/g	932	1,006	986
Maximum possible work out of the system = work/mass (mass), cal	121	805	897
Theoretical work/mass assuming water undergoes constant-volume heating and adiabatic expansion (see Appendix B), cal/g	374	404	396
Maximum adiabatic work out of the system, cal	49	323	360
Measured impulse, 10^4 dyne-sec	0.534	1.82	31.8
Energy based on measured impulse and total salt mass (see Appendix A), cal	0.0043	0.049	15.1
Minimum conversion efficiency = $\frac{\text{minimum measured work}}{\text{maximum theoretical work}}$, %	0.0035	0.0061	1.68
$\frac{\text{Minimum measured work}}{\text{maximum adiabatic work}}$, %	0.0088	0.015	4.19

conversion efficiency formed by determining the ratio of these two values. The conversion efficiency was conservatively low for three reasons: First, the numerator was a lower limit of the actual mechanical-energy release; second, the denominator was calculated on the basis of the maximum expansion work per unit mass of injected water; third, all the water injected up to the time of the expansion was assumed to go through this expansion process, although the movies clearly showed that much of the injected water volume had been expelled from the crucible before the explosion occurred.

A number of conclusions may be drawn from the results of the first test series. High-velocity jets tended to produce only a small early interaction. Low-velocity jets generally produced an even smaller initial reaction, but this was followed, after an inactive delay period, by a secondary explosion of medium or large size. Conservatively evaluated conversion efficiencies as high as ~1.5% were produced in the large-type explosions.

To improve the accuracy of the conversion-efficiency measurement and to gain insight in the manner in which the water-jet velocity influenced the type of interaction, it was necessary to investigate the subsurface interfluid mixing behavior during the delay period between the water injection and an explosion. A second series of tests with various injection pressures was conducted in transparent quartz crucibles so that high-speed movies could record the mixing phenomena in the salt bath.

Some of the second-series tests with water jets of low velocity produced large explosions; the subsurface sequence of events for a typical test of this type is pictured in Fig. 7. The tip of the injection needle was 4 cm above the molten-salt surface. A gas boundary layer built up around the water jet so that it penetrated the salt mass as a long water jet surrounded by an insulating gas envelope. This entrained gas column became unstable, necked down, and allowed contact between the water jet and the salt, resulting in a very small initial interaction. A long delay occurred as the bubble caused by this initial interaction rose to the surface; the salt rushing in behind the bubble totally entrapped a small sphere of water, which then exploded violently. The first column in Table II lists the experimental conditions during this test and gives an accounting of the energy output from the explosion produced by the small entrapped water droplet.

Other tests with low-water-jet velocity produced delayed medium-sized explosions as shown in Fig. 8. The sequence of events again started with the water jet and surrounding gas column penetrating the salt mass until the column formed an instability and generated a small initial interaction. However, the size of the initial interaction was somewhat larger, so that more of the salt was blown out of the crucible and the delayed secondary explosion occurred in a frothy mass at the bottom of an almost empty crucible. The pertinent results from this test are listed in the second column of Table II.

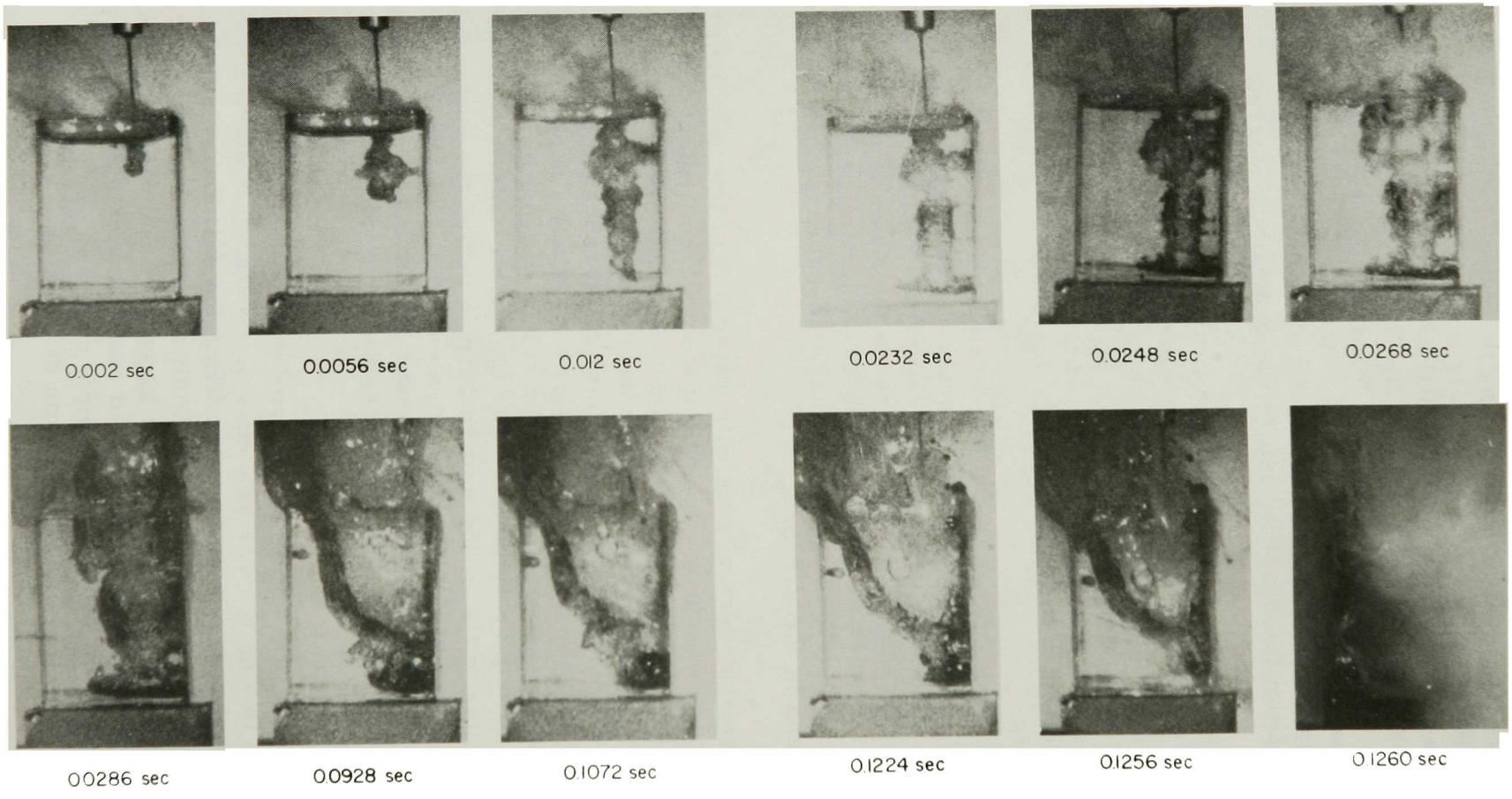

Fig. 7. A Delayed, Large Explosion in a Quartz Crucible. ANL Neg. No. 900-3783.

TABLE II. Energy Account for Tests with Above-surface Injection of Water into Molten NaCl Contained in a Quartz Crucible

Explosion Characteristics			
Time:	Late	Late	Early
Size:	Large	Medium	Small
Salt temperature at time of explosion initiation, T_{in}, °C	1112	1094	1083
Energy in 80 g of NaCl at T_{in}, cal			
Heat in molten NaCl above melt = $mc_p(T_{in} - T_{freeze})$	6839	6444	6203
Heat of fusion = mh_{sf}	9280	9280	9280
Heat in solid NaCl above temperature of boiling water = $mc_p(T_{freeze} - T_{f_{H_2O}})$	14,224	14,224	14,224
Total energy in the NaCl, cal	30,343	29,948	29,707
Injection pressure, psig	7	15	25
Time delay between water-jet penetration and explosion initiation, msec	126	298	7
Volume of injected or entrapped water at time of explosion initiation, cm^3	0.090	2.02	0.048
Theoretical work/mass assuming water undergoes constant-volume heating and constant-temperature expansion at the salt-bath temperature (see Appendix B), cal/g	1149	1134	1125
Maximum possible work out of the system = work/mass (mass), cal	103.5	2291	54.0
Theoretical work/mass assuming water undergoes constant-volume heating and adiabatic expansion (see Appendix B), cal/g	461	455	451
Maximum adiabatic work out of the system, cal	41.5	919	21.6
Measured impulse, 10^4 dyne-sec	13.4	5.0	3.4
Energy based on measured impulse and total salt mass (see Appendix A), cal	7.46	1.05	0.47
Minimum conversion efficiency = $\frac{\text{minimum measured work}}{\text{maximum theoretical work}}$, %	7.2	0.046	0.87
$\frac{\text{Minimum measured work}}{\text{maximum adiabatic work}}$, %	18.0	0.11	2.2

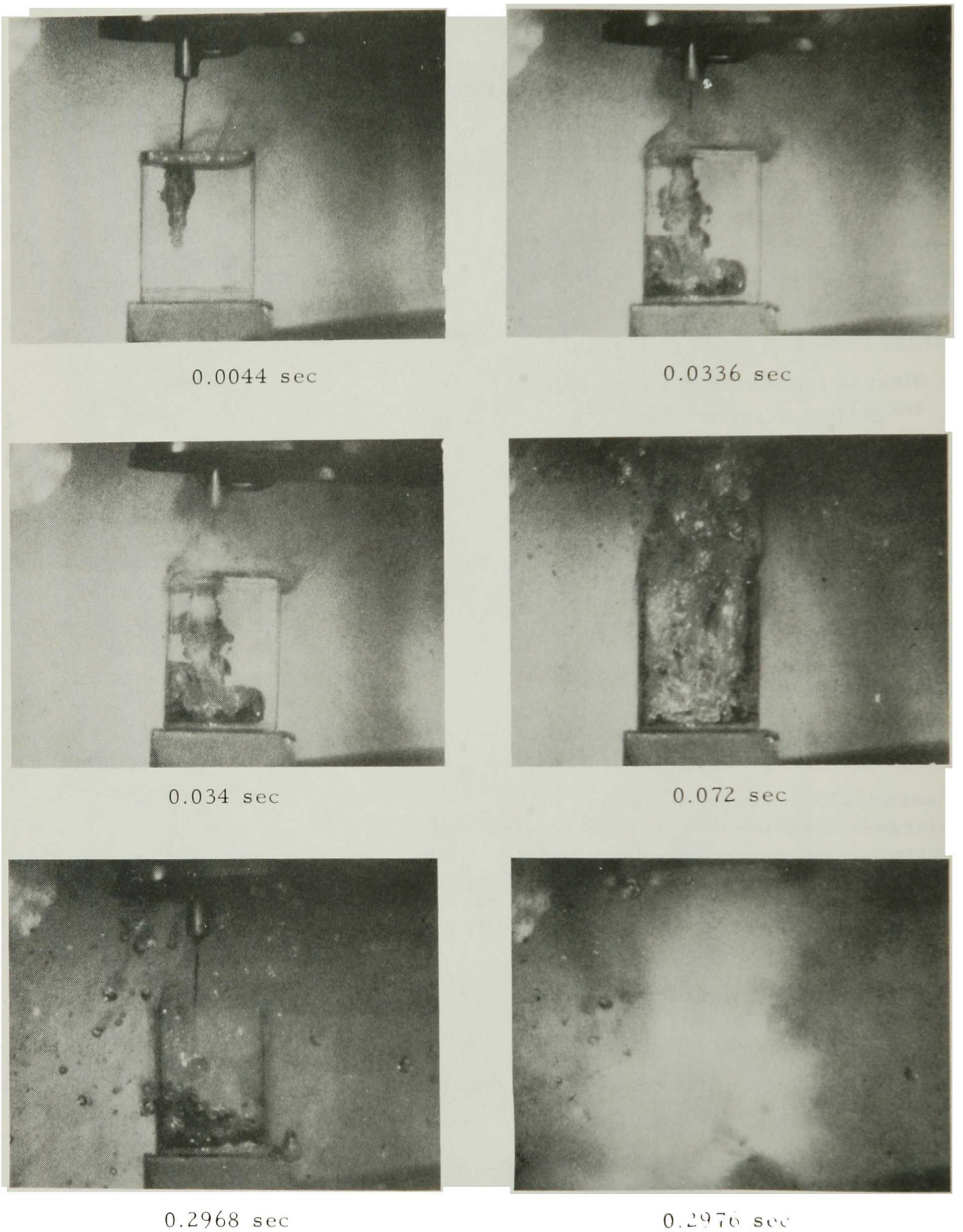

Fig. 8. A Delayed, Medium-scale Interaction in a Quartz Crucible. ANL Neg. No. 900-4499 Rev. 1.

Figure 9 shows selected movie frames from a typical test whose high-velocity water jet produced only an early, small reaction. Once again, an initial interaction was generated by an instability in the gas column surrounding the water jet. The initial interaction for this type of test was large enough to blow virtually all the salt out of the crucible (in some tests, to actually break the crucible), thus effectively preventing any further interaction. Test parameters are listed in the third column of Table II.

The movies were carefully reexamined in an attempt to identify the mechanisms that controlled the growth and collapse of the gas column that in turn acted as a trigger for the initial interaction. Answers were sought for three specific questions: What was the source for the gas in the column? What gas-column parameters determined the size of the initial explosion? How fast did the initial explosion develop?

There were two possible sources for the gas that formed the column. The source could arise from the environment in the blast container if a gas boundary layer built up around the water jet as it crossed the intervening distance between the injection-needle tip and the top surface of the salt mass, or it could come from water vapor boiling off the surface of the water jet as it penetrated the salt mass. The formation of an environmental gas boundary layer was investigated under conditions for which rapid vaporization was impossible, i.e., a cold water jet injected into a cold water mass. Subsurface movies showed that low- and medium-speed water jets produced gas envelopes that penetrated the bulk liquid at the same steady rate and with the same shape in either molten salt or water. (Individual movie frames from the two systems are compared in Fig. 10.) The conclusion was drawn that the gas column formed during tests with low and medium injection pressures consisted mostly of entrained gas with little or no water-vapor component.

Figure 11 shows a high-speed water jet penetrating a molten salt mass. It is evident that there is a different growth pattern for the gas envelope formed around a high-speed jet. When the leading tip of the water jet reached the salt surface, a gas sphere formed and rapidly grew; following a delay, another gas sphere formed and grew immediately below the first sphere; spheres continued to form in this manner until the gas envelope reached the crucible bottom. This behavior suggests that high-speed jets formed surrounding gas columns by rapidly vaporixing the leading tip of the water jet whenever it closely approached or contacted the salt mass.

The delay periods between successive sphere formations were attributed to the transit time for the water jet to cross through the newly formed sphere and again approach the salt mass. The anomalous vapor-volumn formation around high-speed jets was interesting, but not relevant to vapor-explosion research, since tests with high-injection pressures did not produce large explosions; no further experimental studies of such vapor formations were conducted.

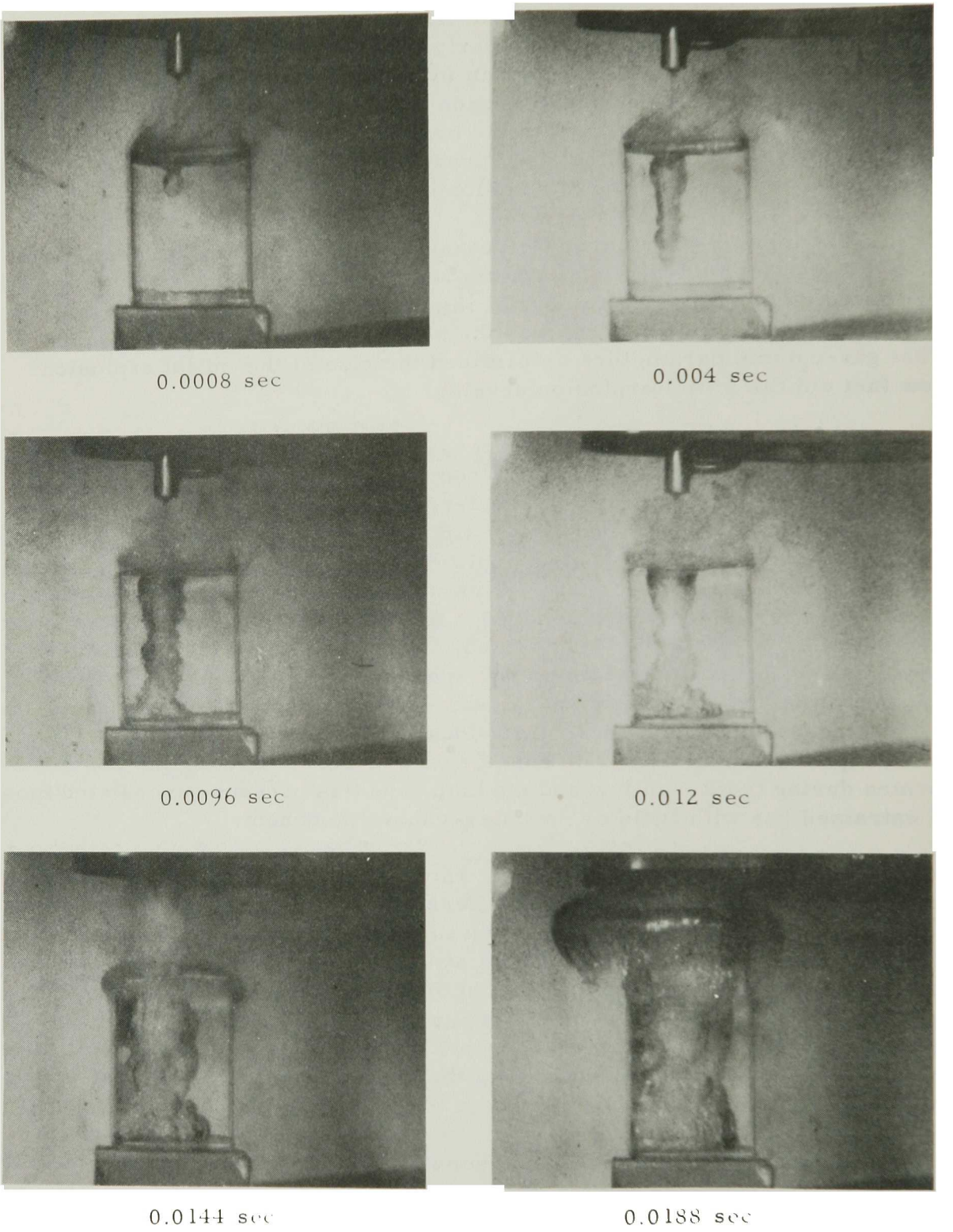

Fig. 9. An Early, Small Interaction in a Quartz Crucible. ANL Neg. No. 900–4498 Rev. 1.

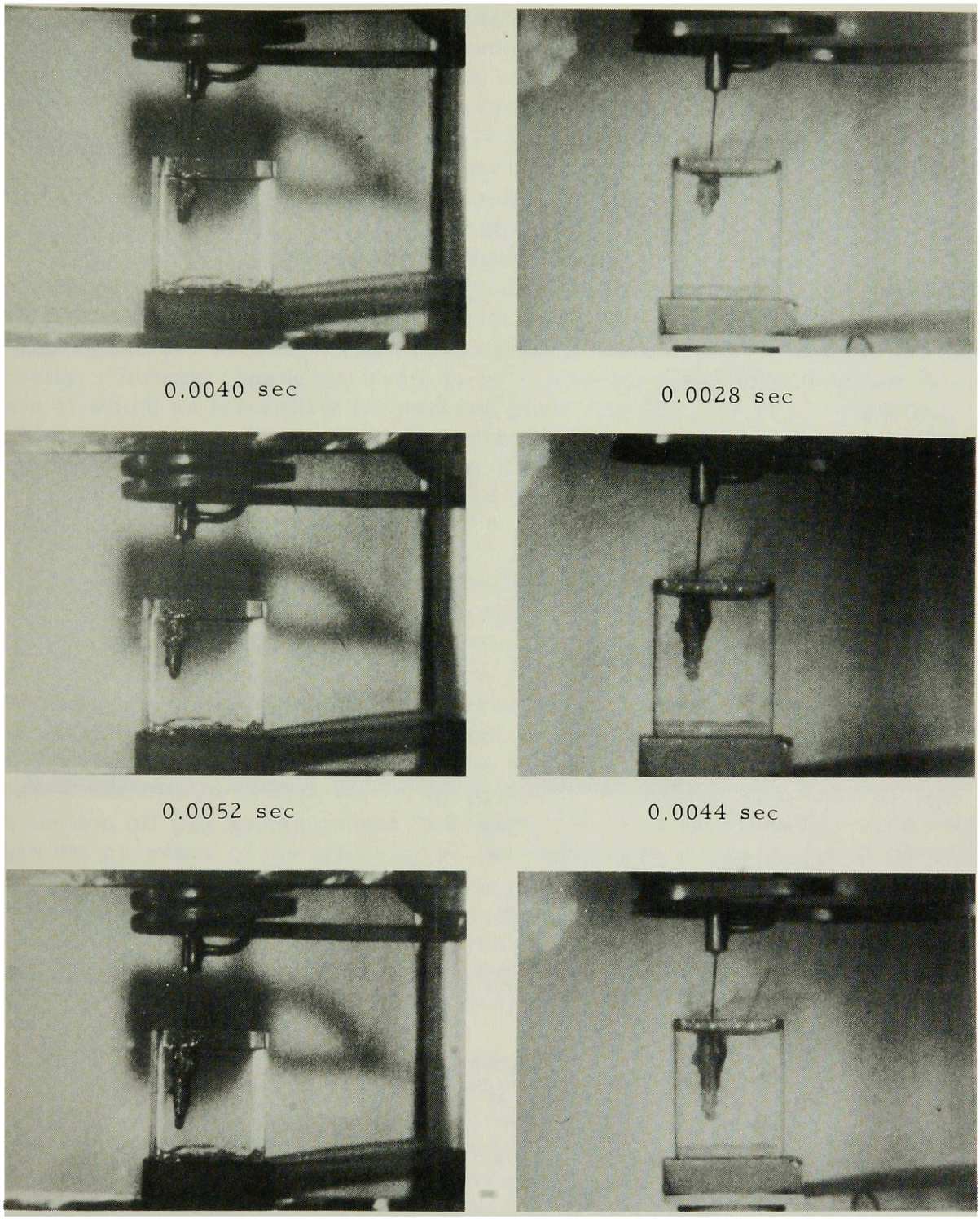

Fig. 10. Comparison of Formation of Entrained Gas Columns Surrounding Two Water Jets as They Penetrated into a Molten-salt Bath and a Water Bath. ANL Neg. No. 900-4533 Rev. 1.

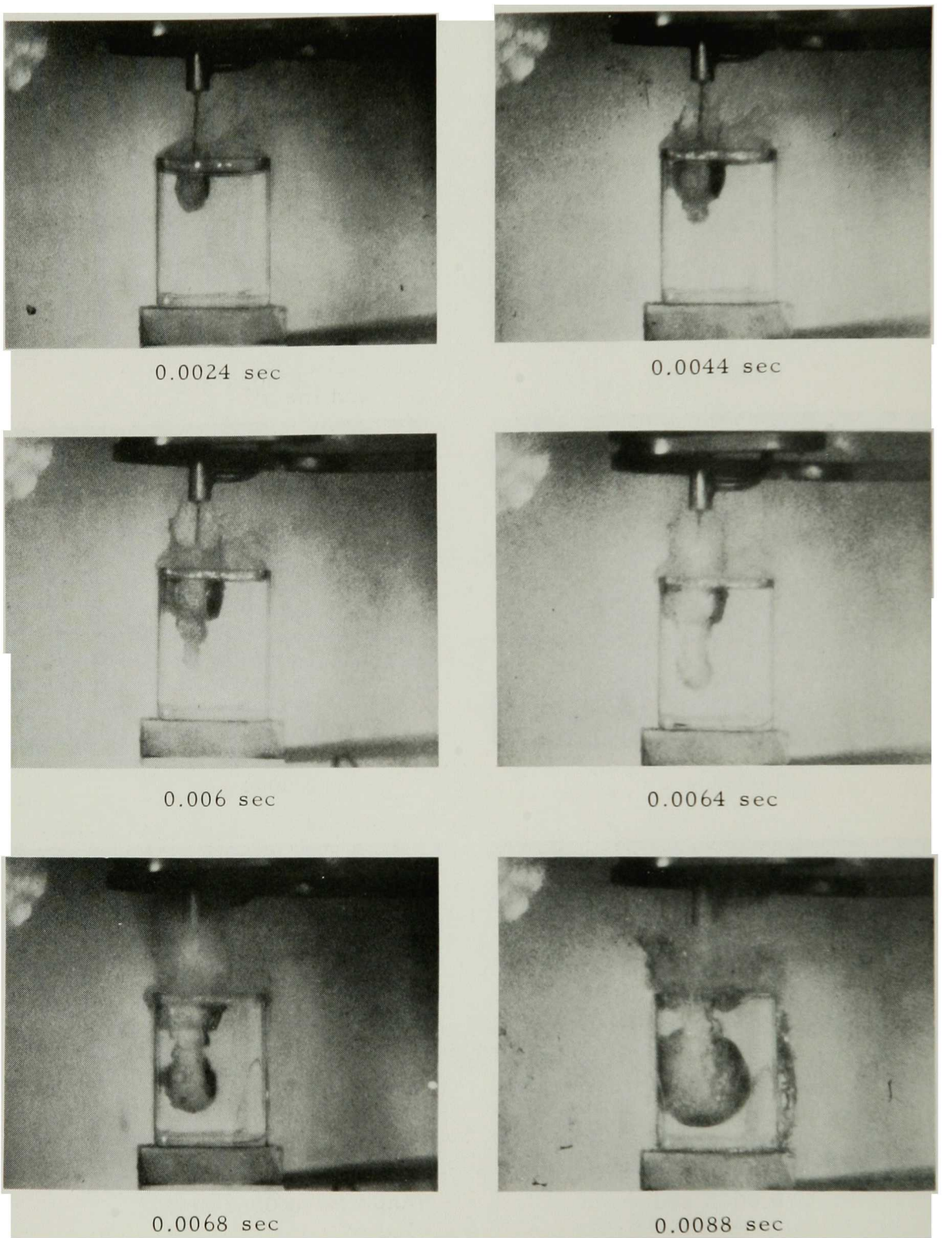

Fig. 11. Growth of Vapor Spheres around the Tip of a High-speed Water Jet as It Penetrated into a Molten-salt Bath. ANL Neg. No. 900-4494 Rev. 1.

Initial interactions were generated when the gas column developed an unstable neck whose rapid closure brought the salt mass into the vicinity of the water jet. Attempts were made to correlate (1) the size of the initial interaction with the vertical location of the unstable neck, (2) the speed at which the neck narrowed down, and (3) the explosive constraint of the salt mass as indicated by the length and diameter of the neck immediately preceding the explosion. Similar explosions resulted from instability formed in various parts of the gas column, indicating that explosion intensity did not correlate strongly with neck location. The velocity of the salt surface inside the rapidly narrowing neck and the minimum neck diameter were interrelated and difficult to measure off the individual movie frames, so that it was impossible to demonstrate an exact correlation between these variables and explosion intensity. However, there did seem to be a general correlation between the rate at which an instability formed and grew, and the size of the resultant initial interaction. This general correlation between constraint and explosion intensity is in agreement with the fact that the geometry with maximum constraint (i.e., a water droplet totally entrapped in the salt mass) produced the largest, most efficient explosions.

Subsurface movies gave two indications when a small explosion occurred: There was a rapid change in the velocity of the gas-liquid interface adjacent to the explosion, and a characteristic white glow appeared in the gas volume surrounding the explosion site. (Although the white glow was very obvious when viewing the original movies, it is not easy to detect in the selected single-frame reproductions used as figures throughout this report. It may be seen at a greatly reduced level in the 0.0-sec frame of Fig. 15 and the 0.0-sec frame of Fig. 14.) This glow was tentatively attributed to light reflection off finely fragmented fluid particles. If this hypothesis were correct, then the presence of the glow inplied the completion of the crucial first-step fragmentation in an explosion sequence, and the rate at which it appeared was an indication of the speed at which the explosion developed. Results from the second test series, in which the movies were taken at 2500 frames/sec and the characteristic white glow always appeared within one frame, gave evidence that the explosions were developing in less that 400 μsec.

In summary, movies taken during the second test series traced the subsurface sequence of events resulting from the impact of both low- and high-velocity water jets into a molten-salt mass, and isolated the sequential variation that caused three different types of explosions. Water jets, of all velocities, entered the salt mass surrounded by an insulating gas layer; the localized collapse of this gas layer produced a small initial explosion whose size and position were determined by the shape of the gas layer. The collapse of gas columns from high-velocity jets tended to produce initial interactions that were large enough to empty the salt from the small crucibles used in these tests, but still small enough to appear subjectively as "small explosions." The low-velocity jets generated two characteristic sizes of mild first interactions. The larger of these two sizes blew most of the salt out of the crucible.

Following a delay, the remaining salt in the bottom of the crucible interacted with the water jet to produce a "medium-sized explosion." The smallest initial interactions produced large subsurface gas bubbles. The turbulent aftereffects of a gas bubble rising through the salt mass occasionally entrapped a water droplet which violently exploded, destroyed the crucible, and appeared as a "large explosion."

The size of the various explosions roughly correlated with the degree of constraint furnished by the surrounding salt mass. The speed of explosive development was too high to follow with 2500-frames/sec movies. Explosions of small entrapped water droplets produced mechanical energy equivalent to at least 7% of the maximum theoretical value.

B. Test Results with Controlled Geometry

Efficient explosions occurred in the parametric experiments when random turbulent fluctuations resulted in a water droplet becoming totally immersed in liquid salt. However, the turbulence that formed this explosive geometry also made it difficult to assess the amount of water available for interaction or to define the explosive containment in the surrounding spongy mixture of molten salt and gas. A second test program was conceived with the goal of producing the same type of geometry in a cleaner system, i.e., a known small quantity of water initially released under the surface of a gas-free molten-salt bath.

In the first test series, water was encased in blown glass spheres, and then these in turn were injected into the salt bath. The spheres were allowed to break from internal pressure generated as the water heated and expanded, or else they were deliberately broken by smashing them into the bottom of the crucible. Two different sequences of events followed the sudden introduction of water below the molten-salt surface. In some of the tests, a very small initial $NaCl-H_2O$ interaction generated a large gas bubble. Both the gas and remaining water buoyantly rose through the salt mass, leaving the system in its final state with water as Leidenfrost drops suspended above a quiescent salt pool. Figure 12 consists of selected movie frames showing this type of behavior.

In other tests, the initial interaction was somewhat more energetic: It either blew the salt out of the intact crucible, or it fractured the crucible itself, as shown in Fig. 13. However, even this larger type of initial explosion was still very small and inefficient when compared with the explosions of water droplets entrapped in the salt by a low-speed water jet. The injection of water-filled glass spheres never produced really large, efficient explosions, for reasons that are presently not clear. The pieces of fractured glass sphere may have impeded mixing and prevented the growth of large-type interactions, or the first step in the fragmentation sequence may have required a large relative velocity between the two liquids to overcome the formation of an insulating vapor layer. Whatever the fundamental cause, the technique failed to produce large, efficient explosions and was, accordingly, abandoned.

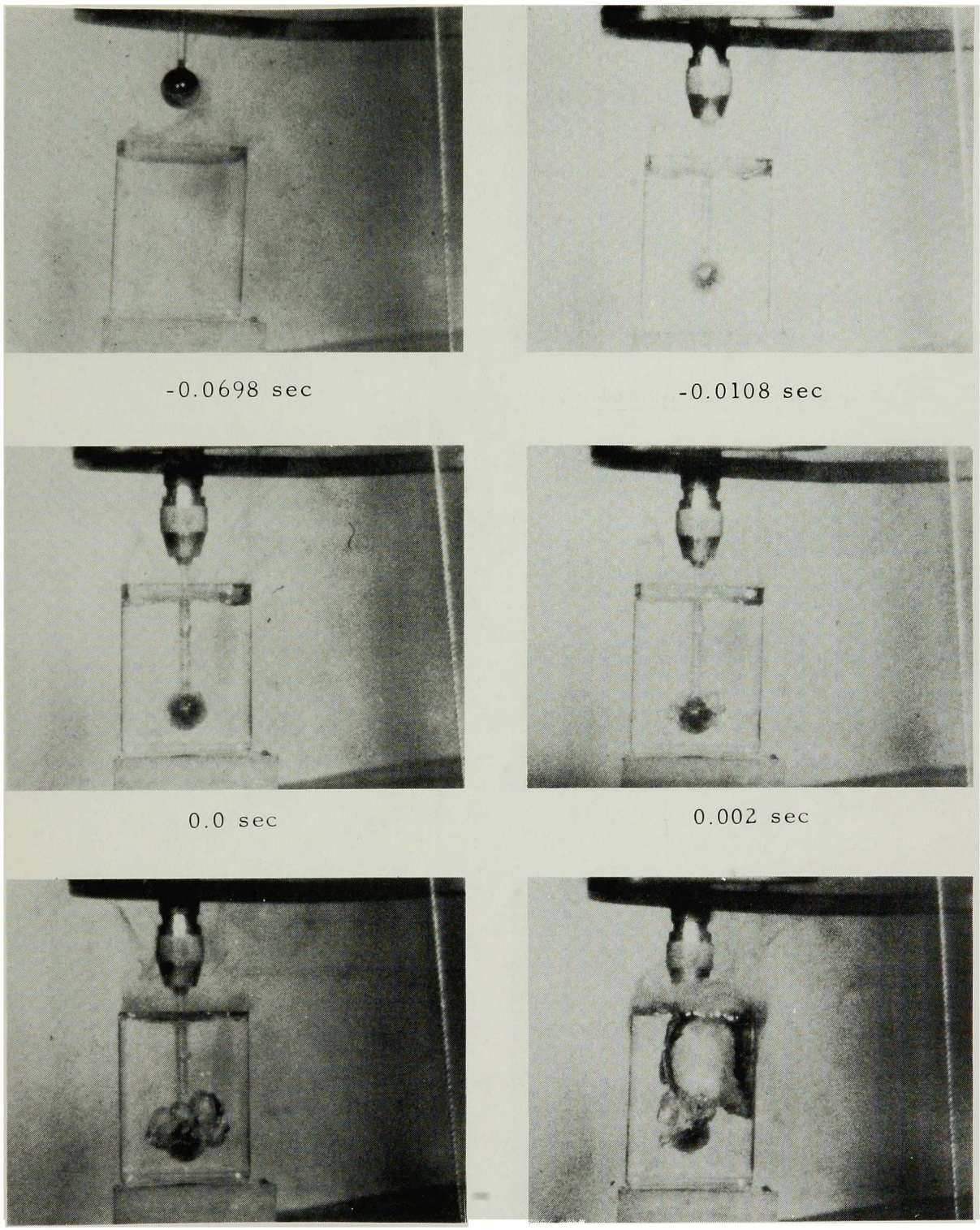

Fig. 12. Bubble Formation Following Rupture of a Water-filled Glass Sphere Submerged in a Molten-NaCl Bath. ANL Neg. No. 900-4497 Rev. 1.

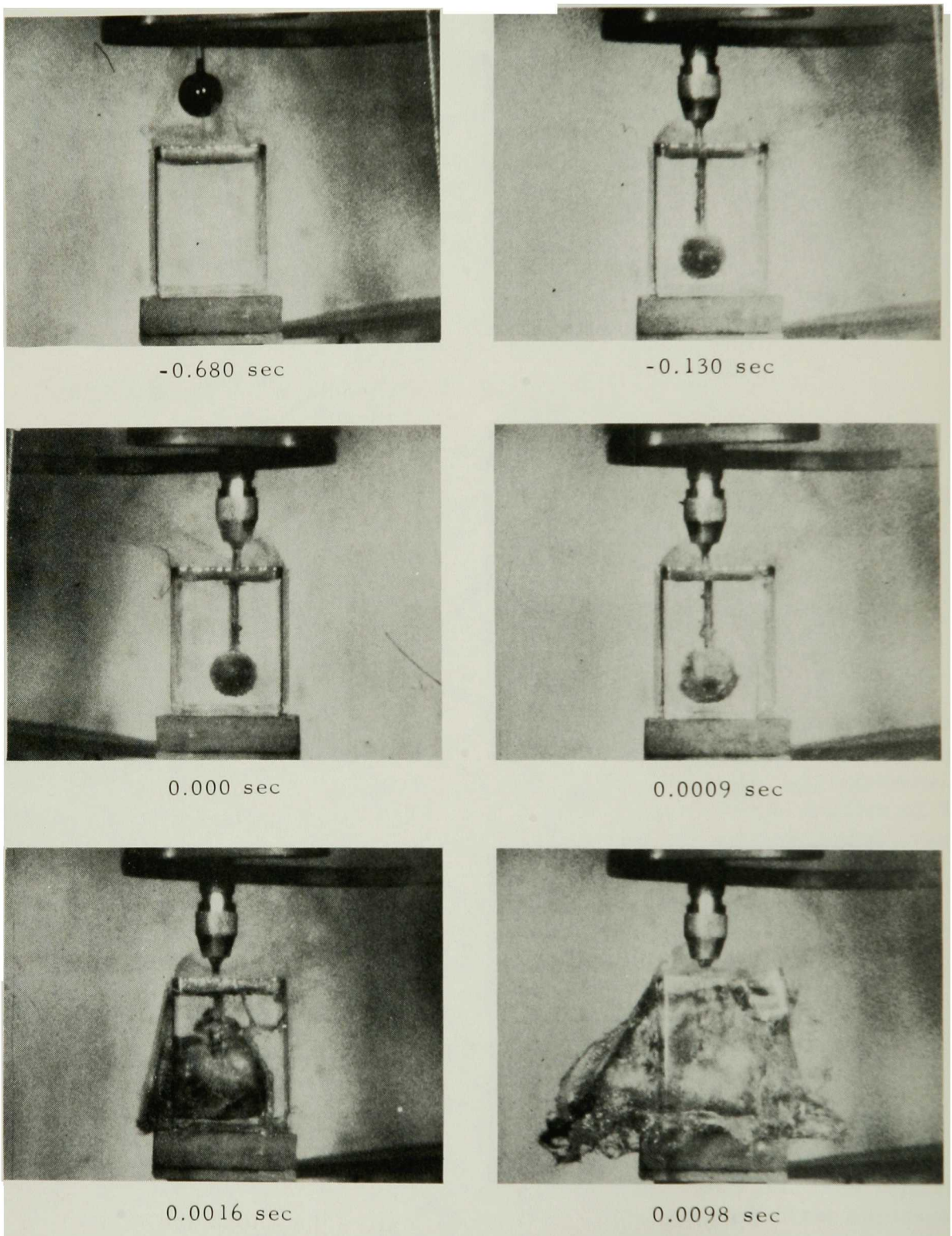

Fig. 13. A Mild Interaction Generated by Rupture of a Water-filled Glass Sphere Submerged in a Molten-NaCl Bath. ANL Neg. No. 900-4495 Rev. 1.

A second series of tests returned to the concept of water injection from a hypodermic needle, but changed the geometry by lowering the needle tip below the molten-salt surface immediately preceding the water injection. Large quantities of water vapor boiled from the needle as it was submerged into the molten-salt bath, causing many of the same problems as in above-surface injection tests. Successive attempts to improve the system by increasing the insulation around the needle finally resulted in a successful test using a needle constructed of concentric quartz tubes with an insulating gas layer between. This system produced explosions with a clean geometry, better controlled measurement of the injected water volume, and a clearer picture of the detailed interaction between the water and the salt.

Selected frames from the first successful submerged ejection test are shown in Fig. 14. Even with a well-insulated needle, a water-vapor bubble formed at the needle tip as it was lowered through the salt bath. Immediately before the water ejection began, the double-walled needle was solidly locked in its lowest position, with a vapor sphere attached to the end of the needle. This vapor was entrained and stretched into a column around the jet as it penetrated into the salt. It took 3.2 msec for the jet and its insulating vapor column to reach the crucible bottom, at which time an explosion initiated. The geometry of the system immediately preceding the explosion was well defined; positioned directly in the center of an otherwise gas-free salt mass was a known amount of water vapor and water. The interacting water and surrounding vapor envelope were in an unusual cylindrical shape with the vertical height about two and a half times as large as the horizontal diameter. This geometry ensured that the major explosive force would appear in a horizontal direction and thus would not register on the load cell which was set up to measure only vertical force components.

The previous method for calculating explosive energy output, as outlined in Appendix A, was based upon the load-cell measurement and an assumed hemispherically symmetrical explosion; it was obviously invalid to apply this approach to the asymmetrical test pictured in Fig. 14. Appendix C describes two alternative methods which may be used to calculate mechanical-energy release. Both methods gave comparable results for the subsurface injection test; the mean value of the two energy calculations is listed along with other experimental variables in Table III. The last entry is labeled "maximum transferred heat." It is a calculated value for the maximum heat that could have been conducted to the water jet if it was in direct liquid-liquid contact with the salt bath for the duration of the time between the ejection of the water and the initiation of the explosion. Since this value is only a small fraction of the measured explosive energy, it may be concluded that most of the destructive energy was transferred between liquids after the initiation of the explosion. This conclusion is very important; it shows that the early conducted heat energy, at most, supplied a triggered mechanism for initiating this explosion.

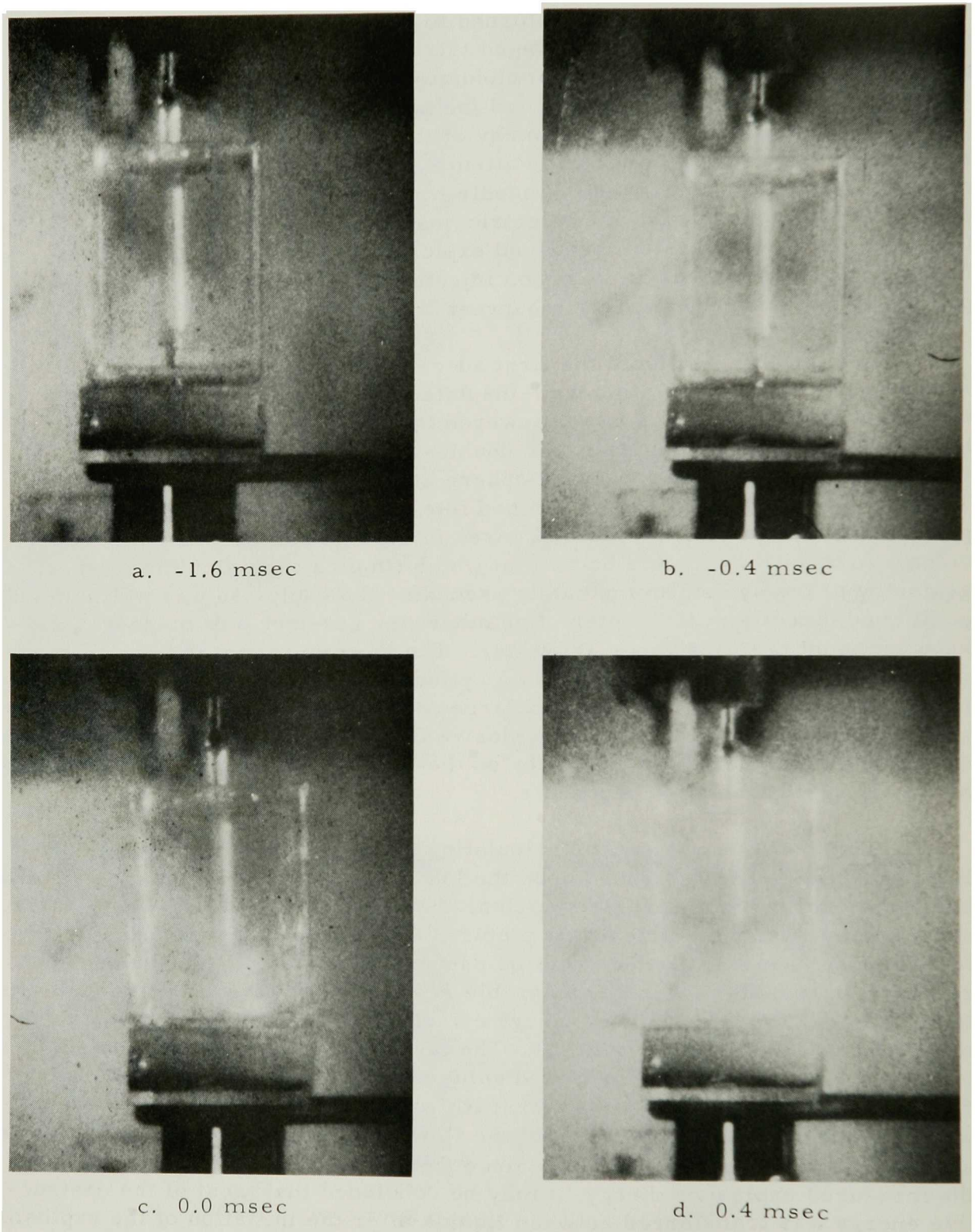

Fig. 14. An Explosion Produced by Subsurface Injection of Water into Molten NaCl; Frames Selected from a Movie Taken at 2500 frames/sec. ANL Neg. No. 900-2727T-1.

TABLE III. Energy Account for Test with Below-surface Injection of Water into Molten NaCl Contained in a Quartz Crucible

Total energy in the NaCl mass	28,460 cal
Volume of injected liquid at time of explosion initiation	0.011 cm^3
Theoretical work/mass assuming water undergoes constant-volume heating and constant-temperature expansion at the salt-bath temperature	1078 cal/g
Maximum possible work out of the system = work/mass (mass)	11.9 cal
Theoretical work/mass assuming water undergoes constant-volume heating and adiabatic expansion	432 cal/g
Maximum adiabatic work out of the system	4.7 cal
Minimum measured energy (see Appendix C)	1.7 cal
Conversion efficiencies	
$\frac{\text{Measured work}}{\text{Maximum work}}$ =	14%
$\frac{\text{Measured work}}{\text{Maximum adiabatic work}}$ =	36%
Maximum transferred heat	0.3 cal

Up to this stage of the experimental program, all the high-speed movies had been taken at 2500 frames/sec and all the efficient explosions had developed in a single frame. It was thought that higher framing speeds might show some of the details of the explosion development. A new lighting system was built and a final series of subsurface-injection tests was run with the camera operating at higher framing speeds. Even at 13,000 frames/sec, the selected movie frames pictured in Fig. 15 show that the initiating explosion developed within one frame (within 77 μsec).

Results from the whole experimental program are summarized in Table IV. Some of the table entries are marked with ---, indicating that the test variables either were not or could not be measured; other entries are marked with ?, indicating that the test measurements were insufficient to specify a range of variables. The exploratory nature of the study made it impossible to exhaustively study all possible experimental combinations. However, the experimental results were broad enough to verify the tabulated major conclusions. These conclusions are compared with various theoretical models in Sec. IV below.

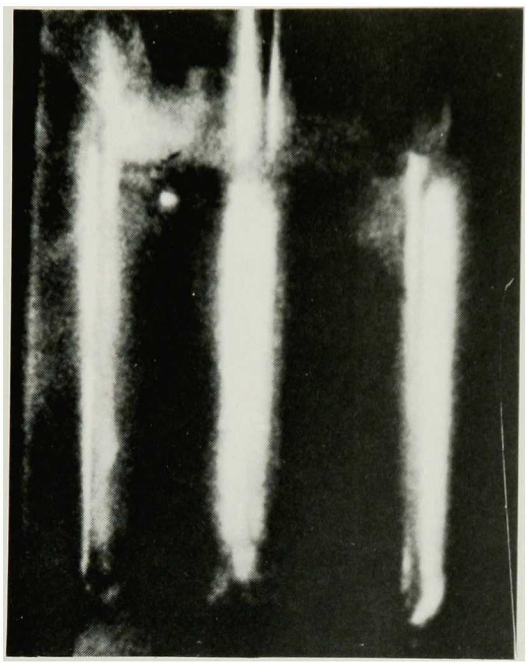

a. -0.08 msec

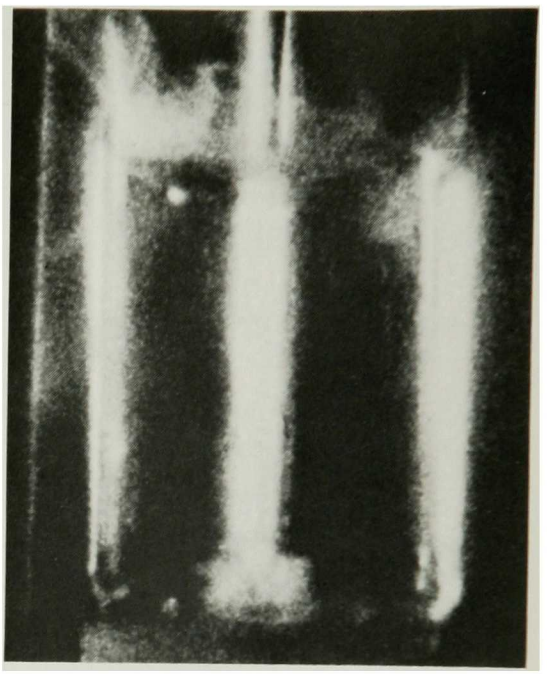

b. 0.0 msec

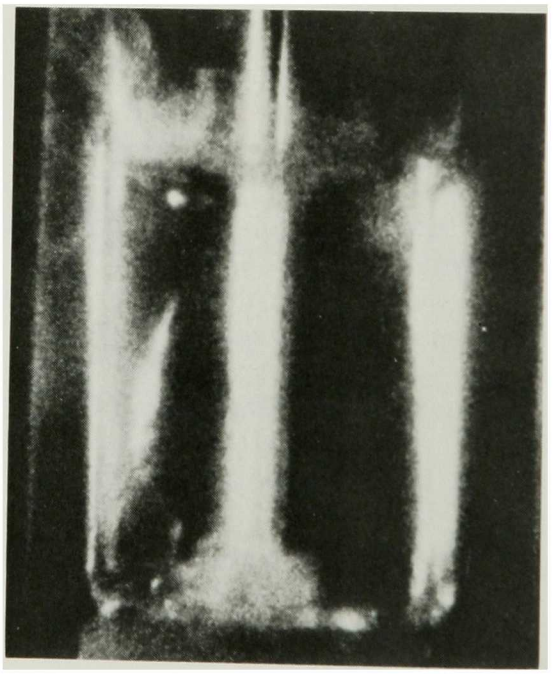

c. 0.08 msec

Fig. 15. An Explosion Produced by Subsurface Injection of Water in Molten NaCl; Frames Selected from a Movie Taken at 13,000 frames/sec. ANL Neg. No. 900-2734T-1.

TABLE IV. Summary of Experimental Results

Fluid-contact Mode	Crucible Material	Injection Pressure, psi	Injection Velocity, ft/sec Above Surface Through Salt	Time Delay between Injection and First Interaction, msec	Measured Impulse of First Interaction, lb_F-sec	Time Delay between Injection and First Interaction, msec	Measured Impulse of Second Interaction, lb_F-sec	Conservative Efficiency = Minimum Measured Work / Maximum Theory Work	Figure Showing Typical Test Behavior	Major Conclusions
Above-surface Water Jet Penetrating Salt Mass	Stainless Steel	60-7	80-30 ---	10-50	0.01-0.1	No secondary explosions occurred in these tests		For first interaction 1% max	4	The existence of three different types of interactions was demonstrated: High injection pressures produced an early, small reaction; low injection pressures produced delayed reactions of medium and large size.
Above-surface Water Jet Penetrating Salt Mass	Stainless Steel	?-7	?-30 ---	10-50	Less than instrument sensitivity	100-300	0.05-0.15	0.15% max	5	
		8-7	~30 ---	10-50	Less than instrument sensitivity	100-300	0.5-0.75	4% max	6	
	Quartz	60-25	80-65 22-18	10-50	Up to 0.05	No secondary explosions occurred in these tests			11	In insulating column of water vapor formed around the water jet as it penetrated the salt mass. Localized collapse of the insulating-gas or water-vapor column generated a small initial reaction whose size determined subsequent system behavior. Relatively large initial reactions dispersed the hot salt mass thus preventing any further interaction. Smaller initial reactions left a frothy salt mass, which again reacted with water to produce a delayed, medium-sized reaction. The smallest initial reaction produced a large vapor bubble, whose trailing turbulence entrapped water droplets in the residual molten salt mass. The entrapped water droplets produced delayed, large explosions.
	Quartz	?-7	?-30 ?-10	10-50	?	No secondary explosions occurred in these tests		?	9	An insulating column of gas was entrained by the water jet as it penetrated the salt mass.
		25-7	55-30 16-10	10-50	Less than instrument sensitivity	100-300	Up to 0.1	0.4% max	8	
		?-7	~30 ~30	10-50	Less than instrument sensitivity	100-300	Up to 0.135	8% max	7	
Water-filled Glass Sphere Injected into Salt Mass	Quartz	---	1	No initial explosions occurred in these tests		No secondary explosions occurred in these tests		---	12	All interactions were prevented by large vapor bubbles which formed around the water mass immediately following rupture of the glass sphere.
Water-filled Glass Sphere Injected into Salt Mass	Quartz	---	0.2-1	---	Up to 0.08	No secondary explosions occurred in these tests		0.02% max	13	The large volume of injected water underwent an inefficient initial interaction which dispersed the molten salt and terminated the test.
Subsurface Water Jet into a Salt Mass	Quartz	7	~7	<5	Up to 0.06	No secondary explosions occurred in these tests		15% max	14	An efficient explosion was produced shortly after the introduction of a water jet below the surface of a quiescent molten salt bath.
Subsurface Water Jet into a Salt Mass	Quartz	7	~7		---	No secondary explosions occurred in these tests		---	15	High-speed movies (13,000 frames/sec) were unable to distinguish stages in the explosive fragmentation; the explosion initiation must occur in a shorter period than the interframe duration (77 μsec).

V. INTERPRETATION OF THE EXPERIMENTAL RESULTS

Section I of this report posed two fundamental questions about vapor explosions and reviewed the information available to answer those questions at the inception of the experimental program. What additional answers may be based on the experimental results reported in the preceding section? Let us consider each question separately.

How much mechanical energy may be released by a vapor explosion? Stated another way, how efficiently can a vapor explosion convert available thermal energy into mechanical energy? Quantitative answers to this question were unavailable before the current test results showed that actual explosions in small-scale equipment could produce energy yields at least as large as ~15% of the maximum theoretical energy yield and ~35% of the calculated yield from a constant-volume-heating/adiabatic-expansion process. These figures are based on very conservative evaluations of the energy output and the interacting liquid volumes, so the actual conversion efficiencies were probably much larger.

Concurrently with this test program, a careful reevaluation of large-scale accidental vapor explosions gave estimated conversion efficiencies of 30-40% of the maximum theoretical yield and 60-70% of the yield from an adiabatic expansion.[10] It seems reasonable to propose, as a best-guess estimate, that the actual energy yield from an efficient vapor explosion will be 50-100% of the yield calculated by assuming the cold working fluid goes through a constant-volume heating process and an adiabatic-expansion process in an equivalent geometric system.

The second fundamental question was: What sequence of events leads to the initiation of a vapor explosion? The answer to this question is not so clear. Obviously the two fluids must be intimately mixed to produce an explosion; the experimental movies showed that the actual mixing process occurred in at least two separate steps, each step requiring mixing on a different volumetric scale. During the preliminary step, the bulk of the two fluids was grossly intermixed, but remained separated from each other by an insulating layer of gas and/or vapor. Eventually this step was terminated when the gas layer developed a localized instability which allowed the two fluids to approach or actually come into contact. Two important explosion parameters, delay period and explosive constraint, were controlled by system behavior during this first step.

The delay period, the time interval between the initial water penetration into the molten-salt mass and the resultant explosion, corresponded to the time required for the appearance and growth of the gas-layer instability. The fluid constraint in the immediate neighborhood of the explosion initiation point was determined by the size and shape of the surrounding gas envelope, which, in turn, was dependent on the preceding bulk-fluid mixing. Experimental results indicate that explosive intensity was strongly influenced by fluid constraint.

Intrafluid contact or near approach initiated the second type of mixing in which some mechanism caused very fine rapid fragmentation and intermixing of the two liquids. Comparison of the measured experimental energy release with theoretical calculations based on a rate-dependent model proved that the fluids must have fragmented into particles with mean radii at least as small as 20 μm,[11] whereas the subsurface movies showed that initial fragmentation must have occurred in times as short as 77 μsec.

The final picture of the vapor-explosion sequence as evolved from the results of small-scale molten-salt-water test contains two steps: an initial bulk-mixing phase, in which the two liquids intermix on a large scale, but remain locally separated by an insulating gas/vapor layer, and a second step, immediately following breakdown of the gas layer, during which the two liquids locally fragment, intermix, and pressurize very rapidly. How do the various hypothesized vapor-explosion mechanisms compare with this picture?

In Sec. I we described four early theories each of which proposed a single mechanism to account for both the first step (delay and bulk mixing) and the second step (fragmentation and pressurization). None of these mechanisms seem consistent with the experimental results. The subsurface movies did not show a frozen shell of salt, as proposed by one theory, nor did they demonstrate that the incoming water jet was fragmented by a Weber-type instability. A simple boiling-regime change, as proposed by a third model, seems a doubtful mechanism, since the experimental behavior and recent theories[12,13] both show the salt-water system was well into stable film boiling. The fourth theory proposed that cold liquid droplets, infiltrated into fissures in a freshly frozen crust of hot material or in the incoming liquid jet of hot material, suddenly boiled and initiated fragmentation. The experimental fact, that some molten metal droplets form spongy masses or bubbles when submerged in water, was cited in support of this fragmentation mechanism. Again the subsurface movies did not show such entrainment behavior, and Epstein[14] has proposed that the bubbling of molten-metal droplets during the cooling process is actually due to the release of absorbed gases.

It may be concluded that none of the early single-mechanism models describe either step in the actual two-step explosion sequence.

Recent theorists have concentrated their efforts on attempts to explain the mechanism that microscopically fragments and intermixes the two liquids following contact at the beginning of the second mixing step. Two generic types of theories have been proposed.

One type of theory (typical examples appear in Refs. 15 and 16) states that some portion of the cold liquid must be heated to a theoretical nucleating limit at which random molecular groupings provide sufficient nucleating sites to locally fracture the liquid and initiate explosive boiling. This boiling is hypothesized to cause sudden pressurization which fragments liquid layers

immediately adjacent to the common intrafluid surface and accelerates the fragmented particles back into liquid-liquid contact. The particles may again be subject to the same sequence of heat, superheating, and sudden boiling, leading to pressurization and even finer fragmentation, or they may transfer large quantities of heat energy through normal conduction and boiling. This intrafluid energy transport, which occurs after the initial fragementation, is known to be an important aspect of vapor explosions, since the results of the subsurface-injection tests proved that a major portion of the energy released by explosions during these tests had been transferred into the cold liquid after the initial contacted fragmentation.

The second type of theory (Refs. 10 and 17, for example) proposes that fragmentation and mixing are caused by dynamic forces working in conjunction with high surface-heat-transfer rates. The high-heat-transfer rates are attributed either to conduction or boiling. Inherent in the boiling phase, as in any system with high-intensity boiling, is some degree of superheat; however, this type of theory does not require that the cold liquid be heated all the way up to its theoretical nucleating limit.

The difference in the required degree of liquid superheat between the two types of theories is an important distinction. The theory that requires superheating to a nucleation limit concludes that certain systems are absolutely prohibited from exploding; the dynamic theory cannot justify such sweeping conclusions.

Both theories have been adjusted to fit all available experimental data. Experiments absolutely proving that vapor explosions do or do not require heating of the cold liquid up to a spontaneous nucleation limit have not yet been conducted.

APPENDIX A

Calculational Procedure for Evaluating Minimum Energy Release from the Measured Impulse

The minimum energy release may be calculated from the measured impulse as follows:

$$\text{Impulse} = I = \int F_z \, dt, \tag{1}$$

where t is time, F is the reaction force, and the subscript z indicates the vertical component. The change in the velocity V of the mass m is

$$\int F \, dt = \int m \, dV. \tag{2}$$

By assuming the accelerating force continuously acts upon the total system mass,

$$I = \int F_z \, dt = m \int dV_z = mV_z. \tag{3}$$

The energy due to the vertical component of the velocity, V_z is

$$\text{Energy}\big|_z = E\big|_z = \tfrac{1}{2} m V_z^2 = \frac{1}{2}\frac{I^2}{m}. \tag{4}$$

Equation 4 may be used to calculate the energy release from the tests with the steel crucibles, since all the reaction force was in a vertical direction. Explosions in quartz crucibles with very little lateral constraint had velocity components in all directions from vertical to horizontal. A conservative way of calculating minimum energy release for this case would be to assume the explosions were hemispherically symmetrical, giving a total energy of twice that due to the vertical component of the velocity:

$$E\big|_{TOTAL} = \frac{I^2}{m}.$$

Note that all the assumptions in this process, i.e., constant mass equal to total system mass and a hemispherical symmetry, give a conservatively low value for the calculated energy release.

APPENDIX B

Calculational Procedure for Evaluating Maximum Mechanical Work Production from the Thermodynamics of the Cold Working Fluid

A vapor explosion rapidly transfers heat from a hot fluid to a cold fluid. The resultant expansion of the suddenly heated cold fluid converts some of the transferred energy into mechanical work, with the remaining energy stored in the cold fluid as internal heat and latent heat of vaporization. The fractional conversion of available energy into potentially destructive mechanical work depends upon the physical properties of the two liquids, the mechanical constraint of the system, and the rate of interfluid heat transfer. The controlling physical mechanisms are poorly understood, thus making it impossible to calculate energy-conversion ratios accurately.

It is possible to specify limiting values for the mechanical-work production using a thermodynamic approach that calculates changes in the internal energy of the cold working fluid as it undergoes a sequence of processes; by hypothesizing the most conservative possible sequence of events we can calculate a theoretical upper limit for the energy conversion. As applied to any general system, this approach requires a continual determination of the internal energy of both fluids during each process. However, for systems such as those involved in the tests described in this report, where the mass of the cold working fluid is very small compared to the mass of the hot fluid, less complicated analytical techniques are required.

Temperature changes in the hot fluid in such a system are too small to have any appreciable effect, and the cold fluid may be assumed to undergo a constant-volume heating up to the temperature of the hot-fluid bath, followed by a constant-temperature expansion back to ambient pressure. Equations for calculating work output will be simplified even further if the constant-temperature expansion is combined with an assumption that the cold fluid may be treated as a perfect gas during the expansion process.

Water will behave almost as a perfect gas as long as the temperature remains well above the critical temperature, and the specific volume is slightly larger than the volume for cold liquid water. Since NaCl freezes at 800°C, the first requirement is certainly to be met in a molten-NaCl-H_2O system. The expansion process starts with the specific volume equal to that of cold water, so that a small error is introduced in this region, but the simplicity of the resulting equations more than compensates for this slight disadvantage. Equations for calculating work produced during the constant-temperature expansion of water treated as a perfect gas may be derived as follows:

$$\text{Work}\Big|_{T=C} = \int P\, dv = RT \int \frac{dv}{v} = RT\, \ell n \frac{v_2}{v_1}, \tag{5}$$

where

v = specific volume,

v_1 = liquid volume for the initial cold water,

$v_2 = RT/P_2$,

R = gas constant,

T = hot-liquid temperature,

P = pressure,

and

P_2 = final expansion pressure.

If the water is assumed to be insulated from the NaCl during the expansion, the isothermal process is replaced by an adiabatic process:

$$Pv^k = \text{constant}, \tag{6}$$

and the work becomes.

$$\text{Work}\big|_{\text{adia}} = \frac{RT}{k-1}\left[1 - \left(\frac{P_2}{P_1}\right)^{(k-1)/k}\right] \tag{7}$$

with the same symbols as in Eq. 5 and

k = ratio of specific heats (assumed constant).

Work calculations based on these equations are compared with experimental measurements in Sec. IV of this report.

APPENDIX C

Calculational Procedure for Evaluating Minimum Energy Release from Measured Radial Velocity and Vertical Impulse

A method of using the measured impulse to determine the minimum mechanical energy released during specific experiments is described in Appendix A. The impulse was measured by a load cell that was sensitive only to vertical force components. The stainless steel crucibles constrained lateral expansion and confined liquid velocity, acceleration, and reaction force to a vertical direction, thus ensuring that the measured value would accurately represent the total impulse produced by an explosion in a stainless crucible. However, the weak quartz crucibles easily fractured and allowed explosive expansion in all directions, thus necessitating some additional assumptions to assess the total impulse and kinetic energy from the measured vertical components.

In Appendix A, the existence of a hemispherically symmetrical explosion was assumed, and the derived results were applied to test cases for which this assumption seemed reasonably correct. However, the subsurface injection of water into a molten salt mass produced a very asymmetrical explosion. Figure 16 is a graphical picture of the experimental conditions in one specific test immediately preceding the explosion initiation. Pressurization of the long narrow gas cavity that surrounds the liquid jet would produce an initial horizontal force ~10 times as large as the initial vertical force (directly proportional to the relative surface areas). Two methods for assessing energy release from asymmetrical explosions are outlined below.

REXCO is a computer code that may be used to calculate the dynamic response of a liquid mass to the sudden pressurization of a contiguous gas volume. It requires, as input, the specification of the shape of the individual liquid-volume segments, the equation of state of both gas and liquid, and the initial condition of the pressurized gas; the output lists new boundaries, velocities, and pressures for each liquid-volume segment, and the total kinetic energy summed over all volume segments, for every specified time increment. The code was used to calculate the response of a system whose experimental geometry is pictured in Figs. 14 and 16 during the first 0.00150 sec after sudden gas pressurization; these results, in turn, allowed evaluation of the proportionality constant between the total kinetic-energy production and the square of the vertical component of the impulse; finally, this constant was combined with the measured impulse to determine the actual kinetic energy released during the first 0.0015 sec as about 5.0 ft-lb_F. Kinetic energy released over the whole liquid-expansion period should be somewhat larger.

An alternative method of assessing experimental energy release is based on the velocity at the surface of the expanding liquid volume as measured from successive movie frames. This approach gave a kinetic-energy release of 5.3 ft-lb_F for the test pictured in Figs. 14 and 16. Again, this

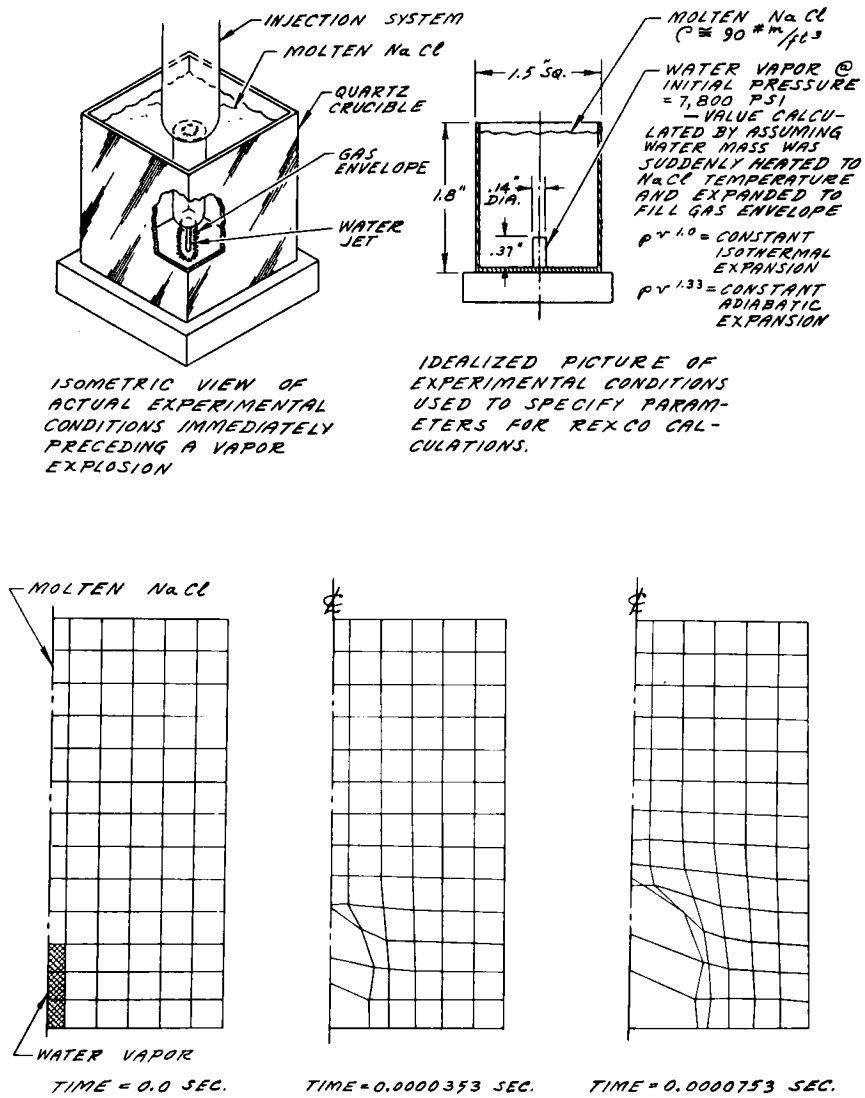

Fig. 16. Experimental Conditions and REXCO Calculations of System Expansion following Vapor-explosion Initiation. ANL Neg. No. 900-4486 Rev. 1.

number is expected to be somewhat lower than the actual energy release, since the liquid velocity has to be evaluated at its minimum point on the outside surface of an expanding spherical shell.

The "Minimum Measured Energy" listing in Table IV is an average value from the above two results.

REFERENCES

1. W. Nelson, Combustion Engineering, Inc., Windsor, Conn., personal communication.
2. S. G. Lipsett, *Explosions from Molten Materials and Water*, Fire Tech. *2*, 118-126, Boston (1966).
3. G. Long, *Explosions of Molten Aluminum in Water*, Metal Progress, p. 107 (May 1957).
4. W. Nelson and E. H. Kennedy, *What Causes Kraft Dissolving Tank Explosions*, Paper Trade J. *140*, 29 (July 16, 1956).
5. G. P. Hicks and D. C. Menzies, "Theoretical Studies on the Fast Reactor Maximum Accident," *Proc. Conf. Safety, Fuels, and Core Design in Large Fast Power Reactors*, ANL-7120, pp. 654-670 (Oct 1965).
6. A. Padilla, Jr., *Transient Analysis of Fuel-sodium Interaction*, Trans. Am. Nucl. Soc. *13*, 375 (1970).
7. D. H. Cho, R. O. Ivins, and R. W. Wright, "Pressure Generation by Molten Fuel-coolant Interactions under LMFBR Accident Conditions," *Proc. Conf. on New Developments in Reactor Mathematics and Applications, Idaho Falls*, USAEC CONF-710302, pp. 25-49 (Mar 29-31, 1971).
8. D. R. Armstrong and D. H. Cho, "Simulation Experiments of Coolant Entrapment in Molten Fuel," *LMFBR Nuclear Safety Program Annual Report: July 1, 1969, to June 30, 1970*, ANL-7800, pp. 349-358 (July 1971).
9. R. O. Ivins, ANL, personal communication.
10. R. P. Anderson and D. R. Armstrong, "Comparison Between Vapor Explosion Models and Recent Experimental Results," *Fourteenth National Heat Transfer Conf.*, AIChE-ASME, Atlanta, Ga. (Aug 5-8, 1973).
11. D. H. Cho, ANL, personal communication.
12. K. J. Baumeister and F. F. Simon, *Leidenfrost Temperature--Its Correlation for Liquid Metals, Cryogens, Hydrocarbons, and Water*, J. Heat Transfer, pp. 166-173 (May 1973).
13. R. E. Henry, *A Correlation for the Minimum Wall Superheat in Film Boiling*, Trans. Am. Nucl. Soc. *15*(1), pp. 420-421 (June 1972).
14. M. Epstein, *Thermal Fragmentation--A Gas Release Phenomenon*, Nucl. Sci. Engr. *55*, 462 (1974).
15. T. Enger and D. Hartman, *Proc. Third Int. Conf. Liquefied Natural Gas*, Washington, D. C. (1972).
16. H. K. Fauske, "Some Aspects of Liquid-Liquid Heat Transfer and Explosive Boiling," *Proc. Fast Reactor Safety*, USAEC CONF-740401 (Apr 2-4, 1974).
17. S. J. Board, C. L. Farmer, and D. H. Poole, *Central Electricity Generating Board Report*, RD/B 12423 (1972).